Low-frequency variability of atmospheric planetary waves Part I: observations and mechanisms

Franco Molteni
European Centre for Medium-Range Weather Forecasts

Rayleigh-Benard convection

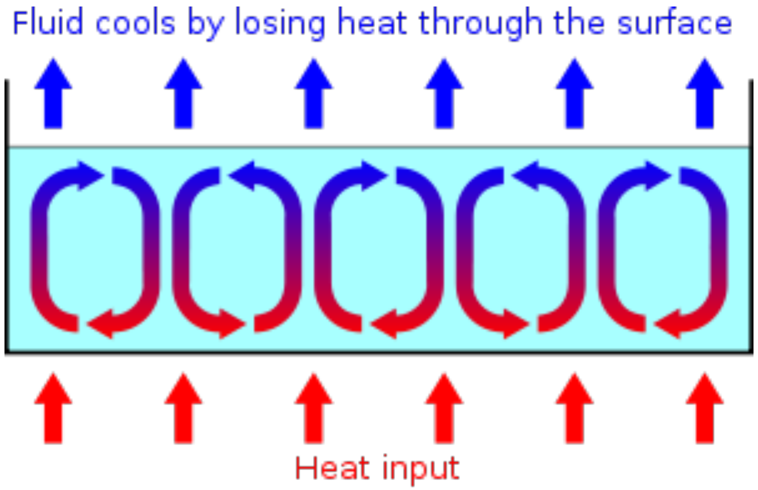

Fluid temperature

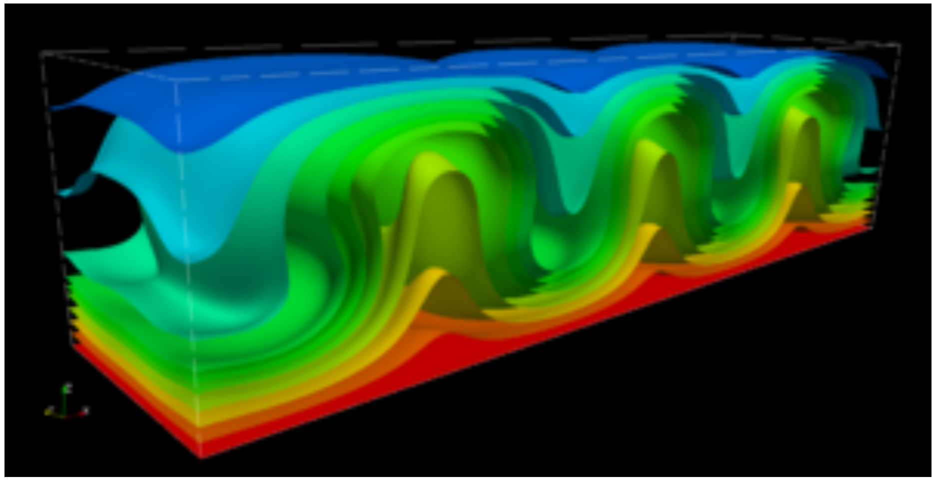

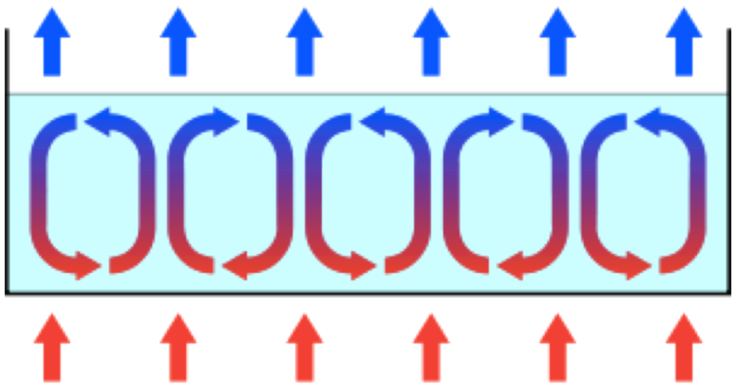

If the rotation of the convective cells is reversed, the upward heat flux is the same

Planetary waves in Jan: geop. height 500 hPa

geop.h. 500 hPa jan1984

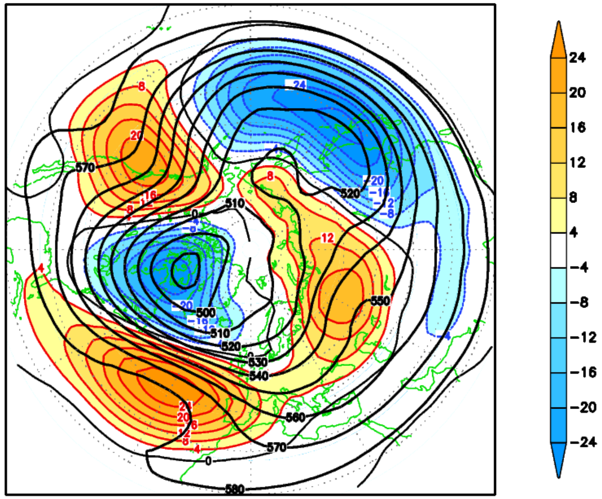

geop.h. 500 hPa jan1989

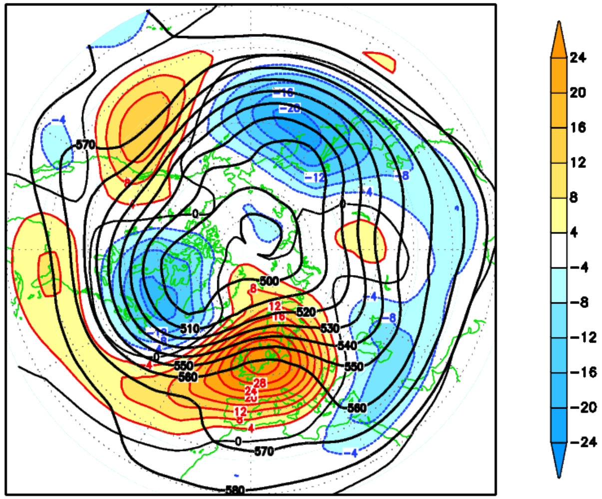

geop.h. 500 hPa jan1985

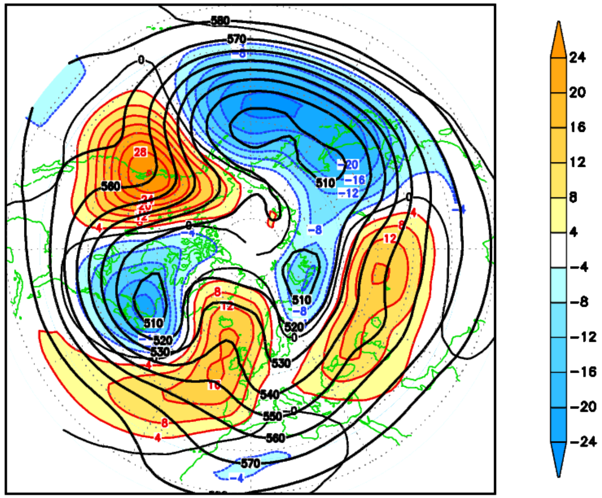

geop.h. 500 hPa jan1996

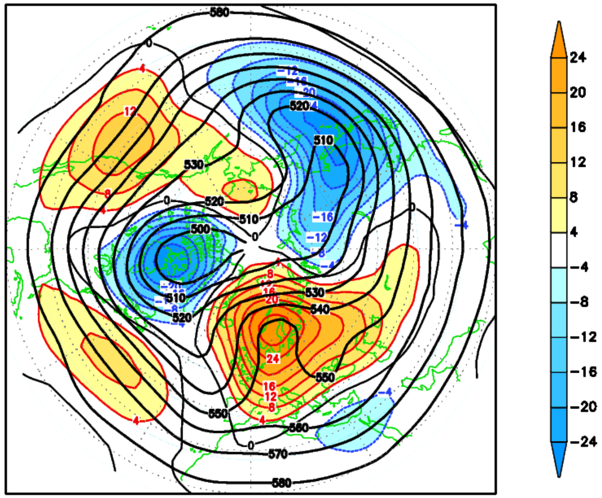

Planetary waves in Jan: eddy T and v-wind 850 hPa

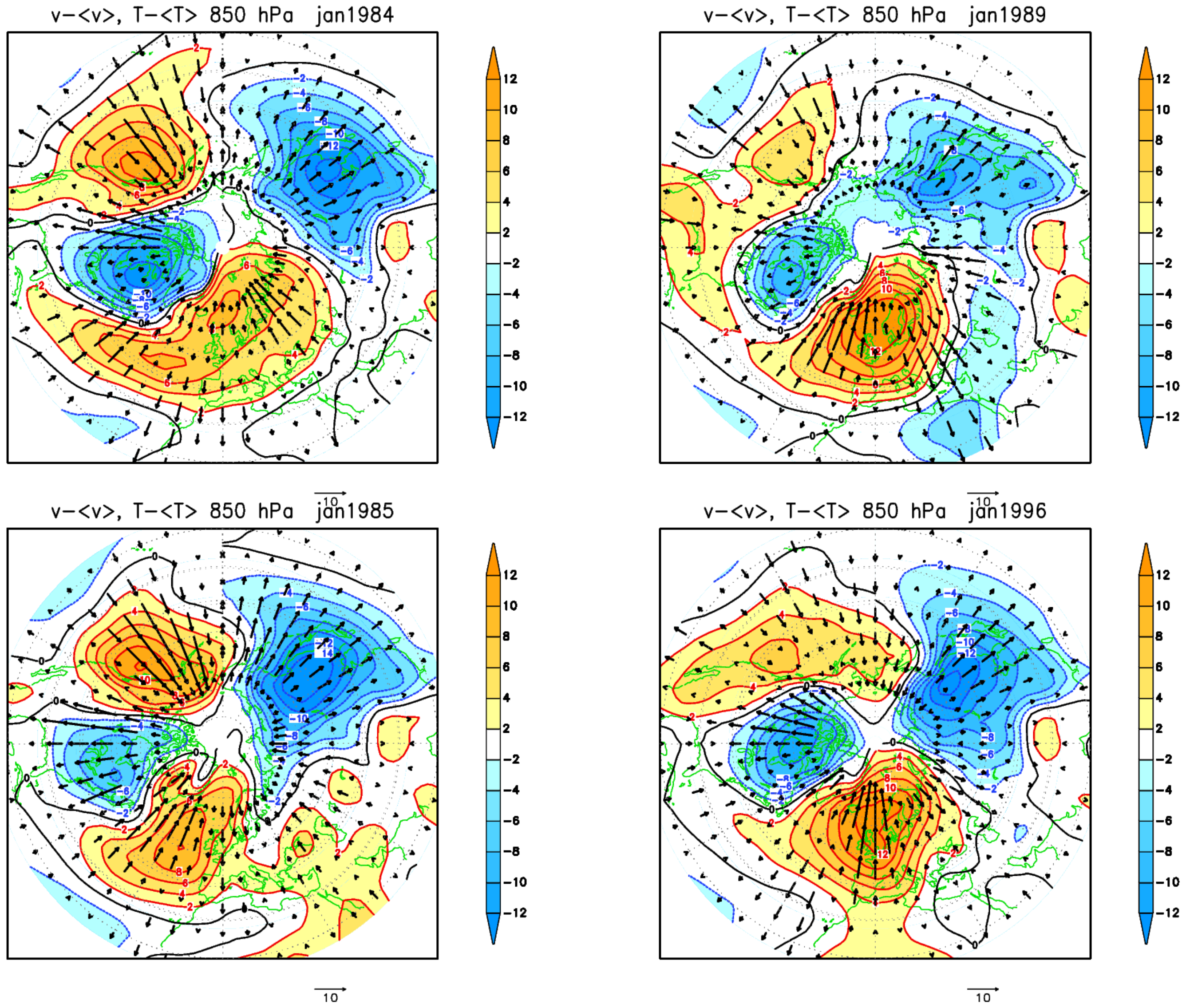

Modes of large-scale variability: ENSO

The El Niño - Southern Oscillation

Walker and Bliss (1932); Bjerknes (1969)

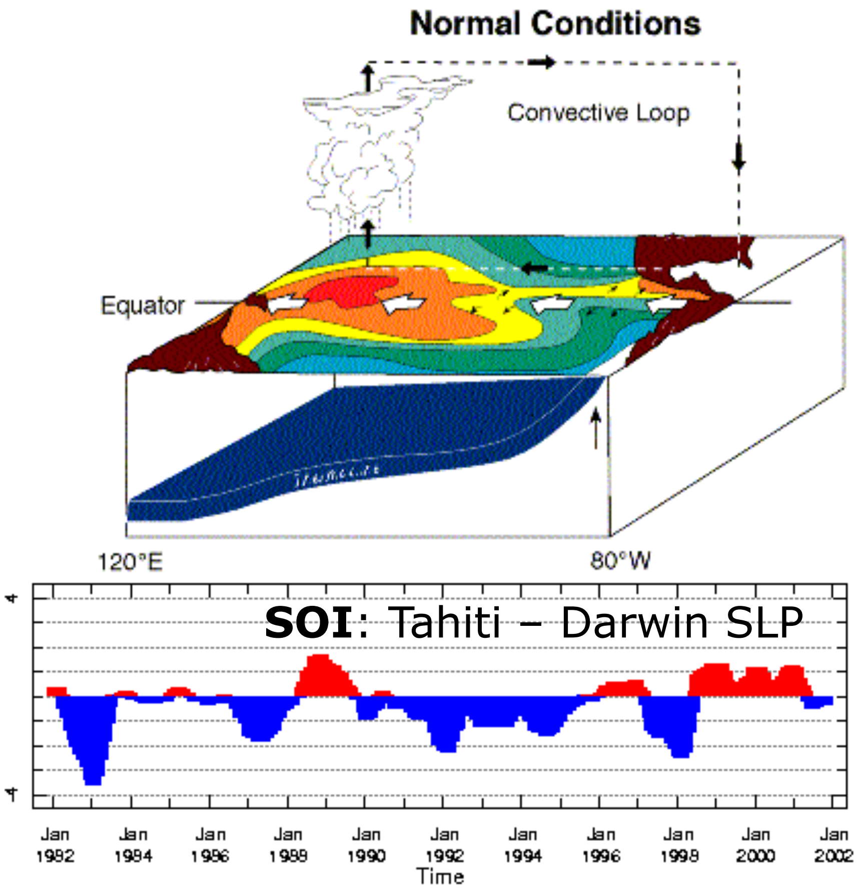

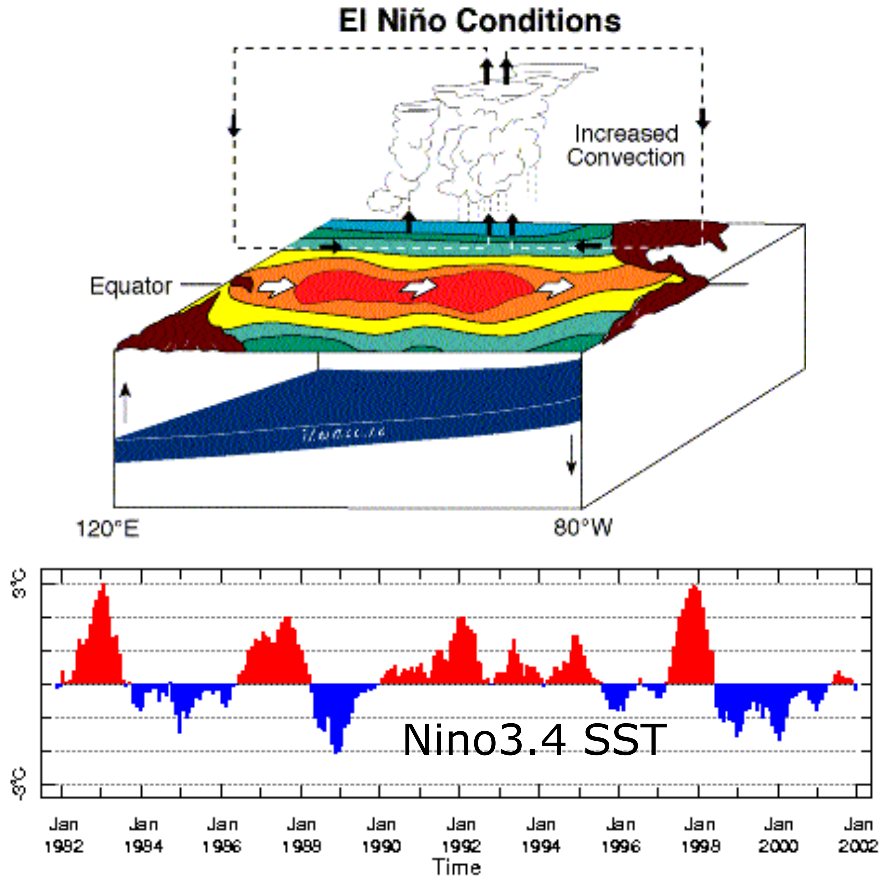

ENSO teleconnections: rainfall and temperature

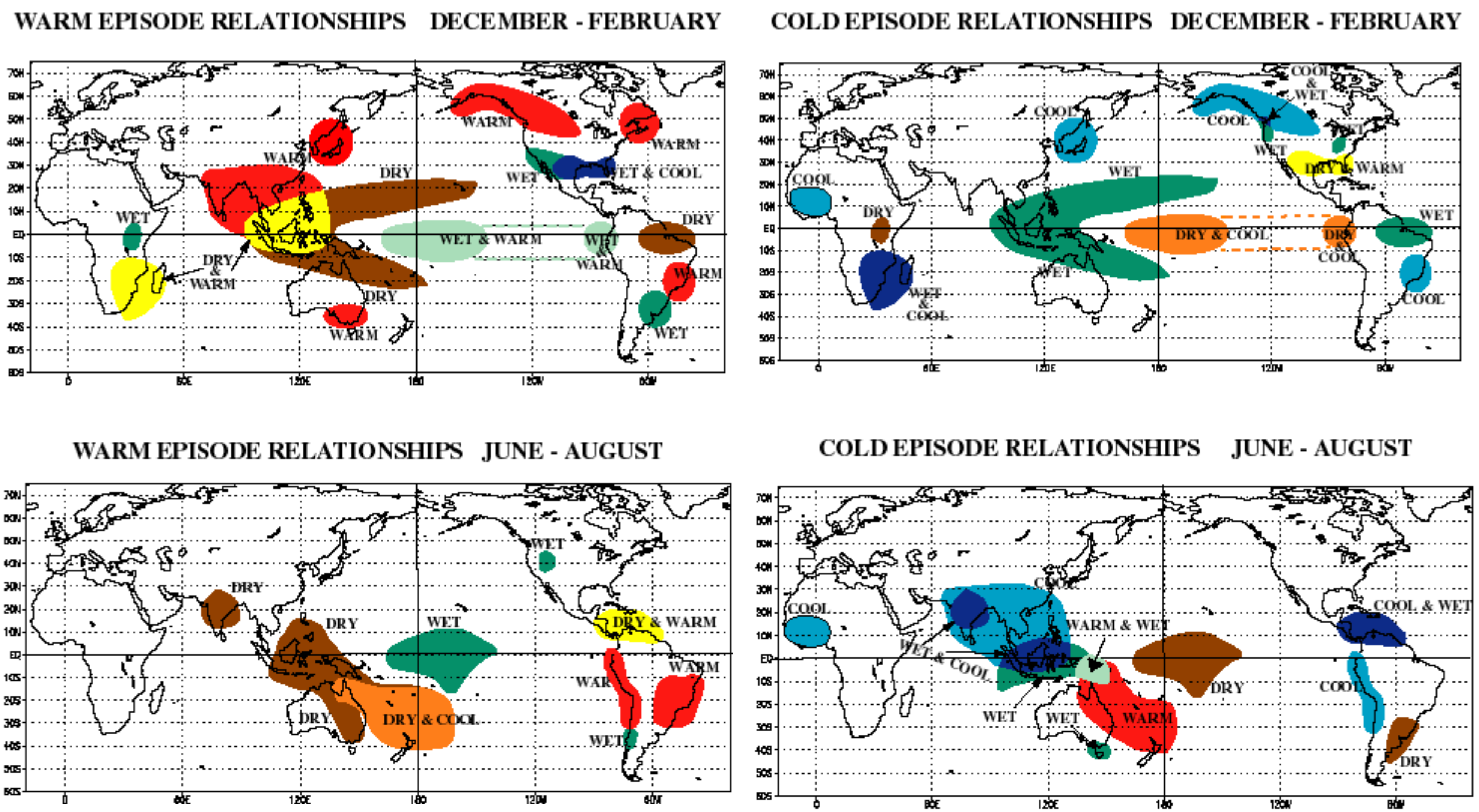

Modes of large-scale variability: NAO

The North Atlantic Oscillation

Walker and Bliss (1932)

Van Loon and Rogers (1978)

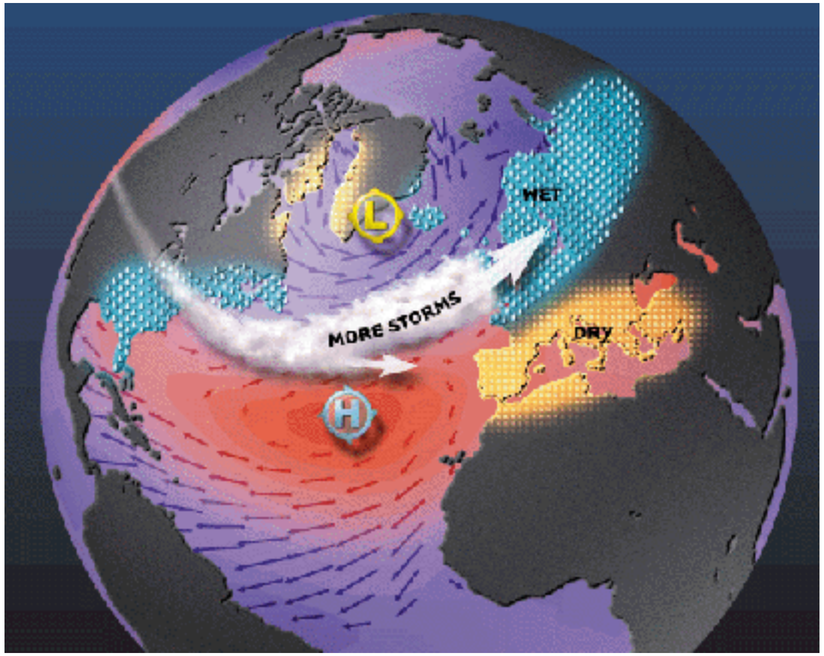

Positive NAO phase

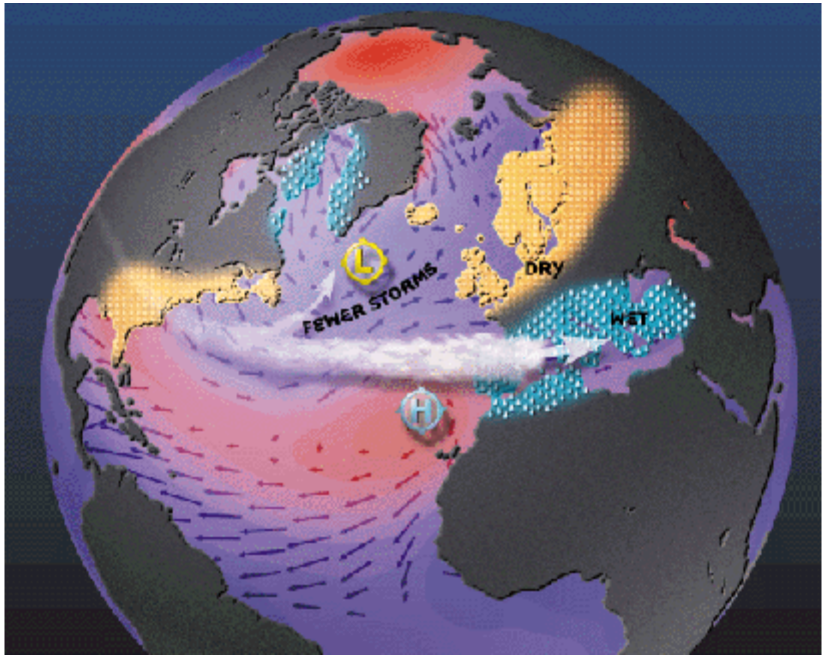

Negative NAO phase

Teleconnection patterns: Wallace and Gutzler 1981

The Pacific / North American (PNA) pattern: correlations

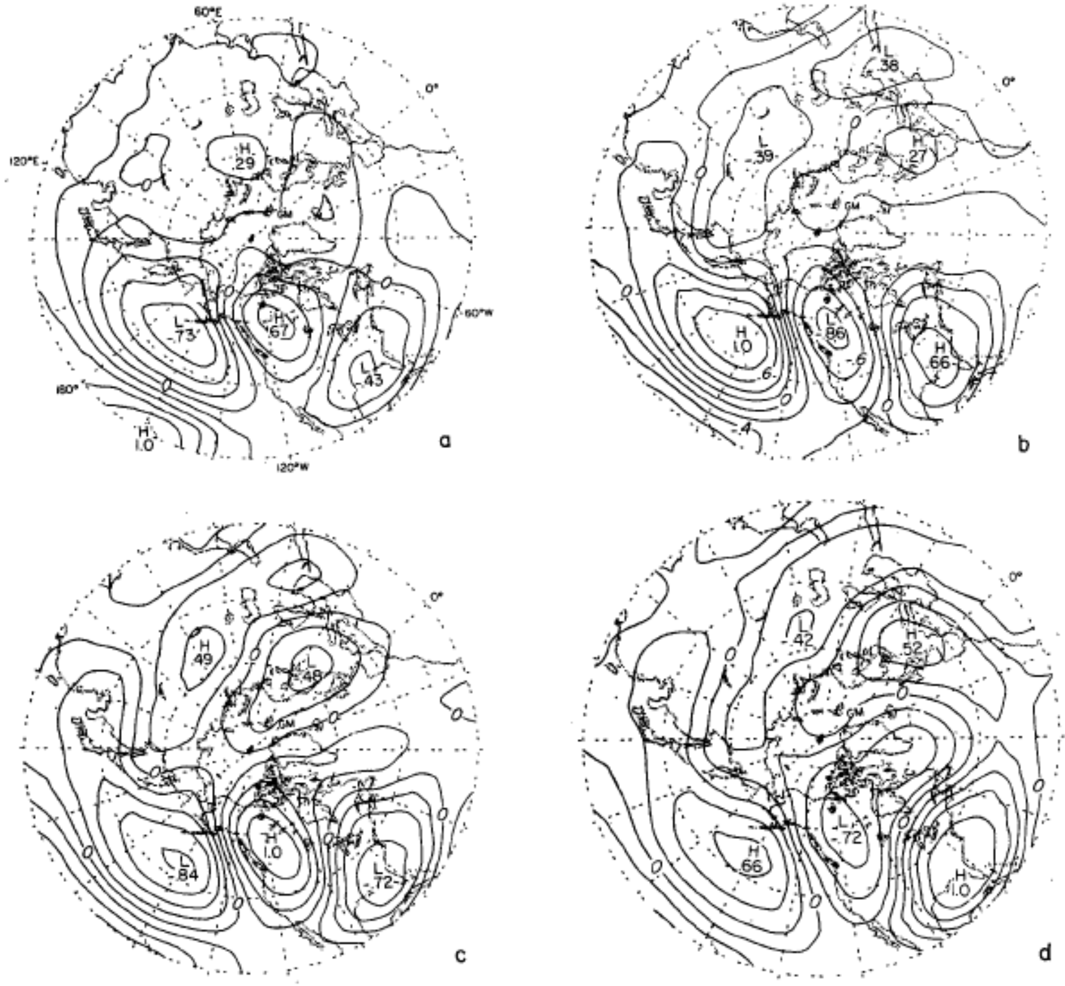

FIG. 16. As in Fig. 12, but for base grid points (a) 20°N, 160°W; (b) 45°N, 165°W; (c) 55°N, 115°W; (d) 30°N, 85°W.

Teleconnection patterns: Wallace and Gutzler 1981

The Pacific / North American (PNA) pattern: composites

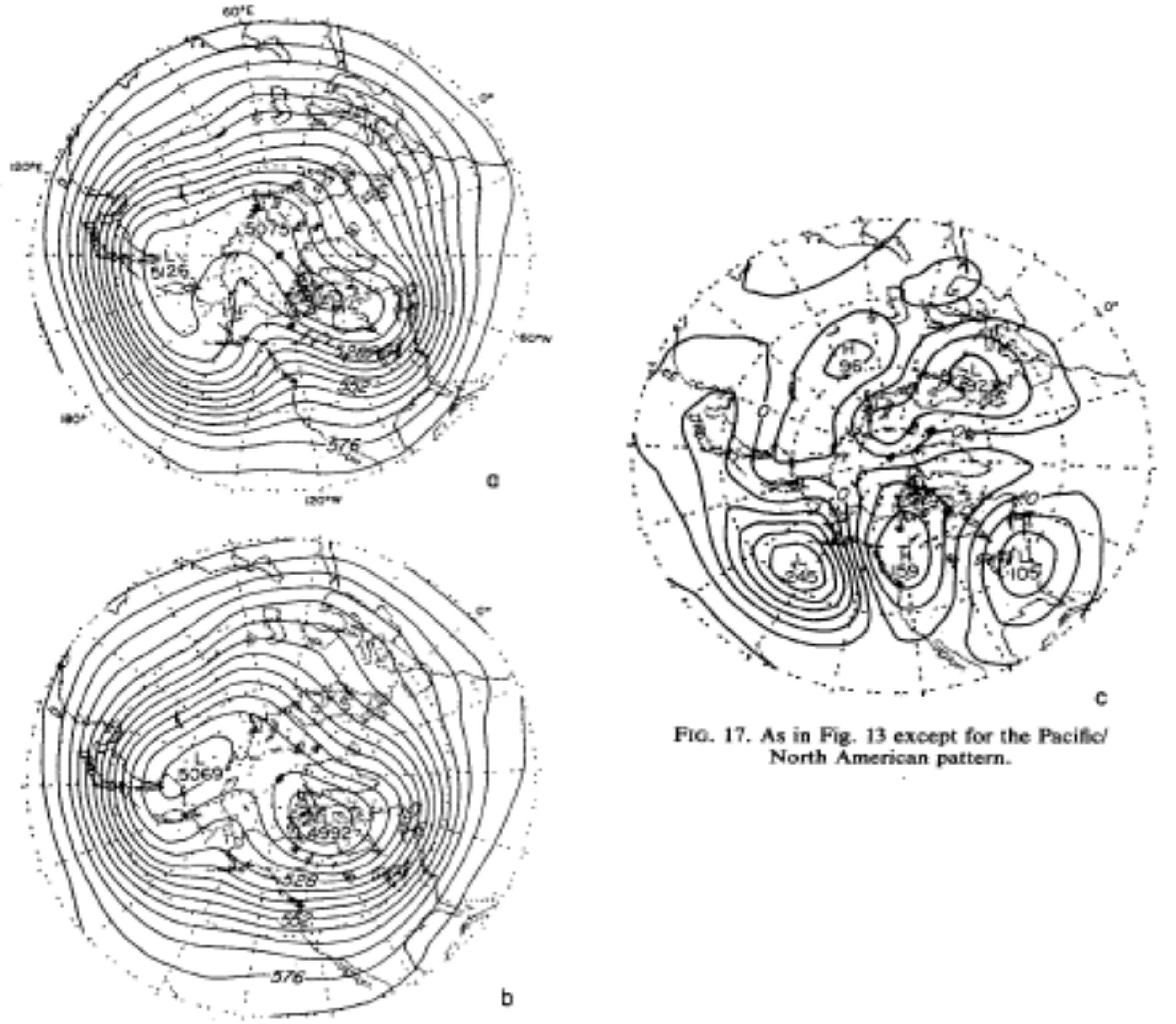

FIG. 17. As in Fig. 13 except for the Pacific/ North American pattern.

Teleconnection patterns: Wallace and Gutzler 1981

Eastern Atlantic (EA) pattern: composites

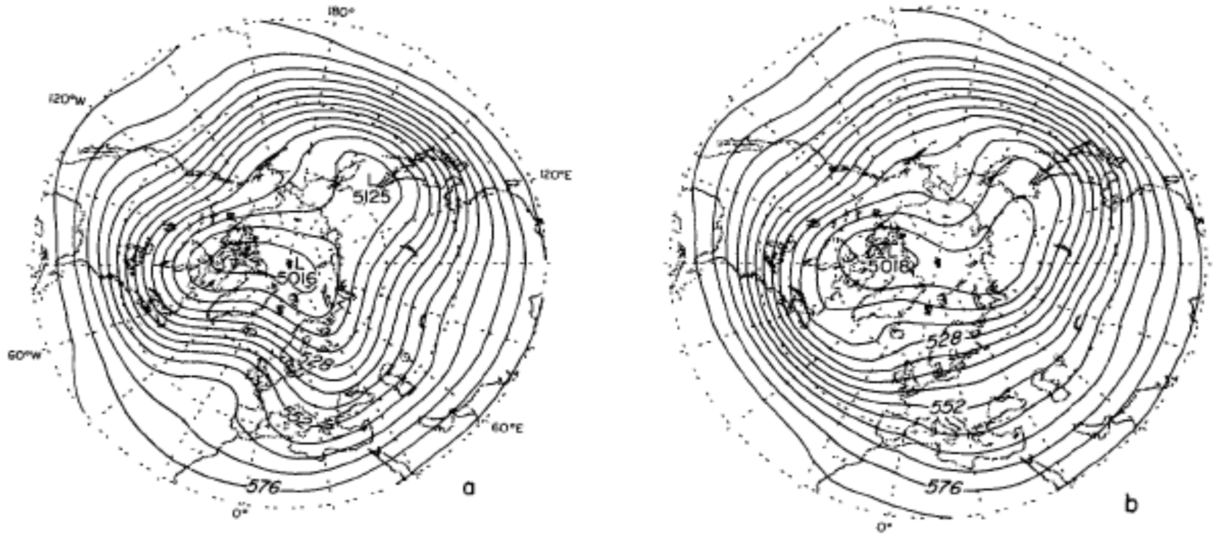

FIG. 13. Composite 500 mb height charts based on the 10 months out of the 45 month data set with the strongest (a) positive and (b) negative values of EA. Contour interval is 60 m. (c) Composite chart (a) minus composite chart (b), contour interval is 40 m.

Understanding teleconnections: Horel and Wallace 1981

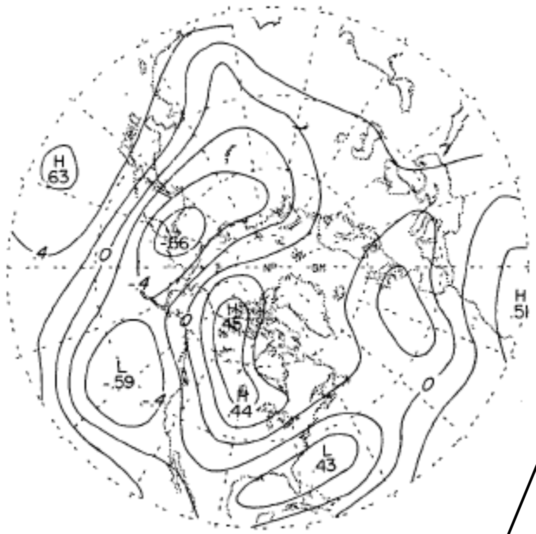

a

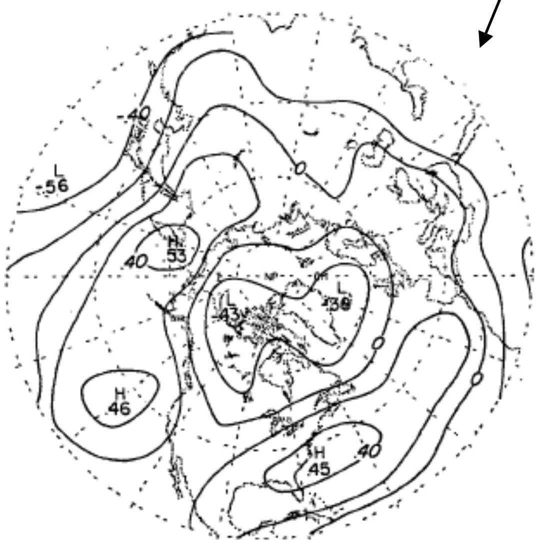

c

Correlation of 700hPa height with
a) PC1 of Eq. Pacific SST
c) SOI index

Schematic diagram of tropical-extratropical teleconnections during El Niño

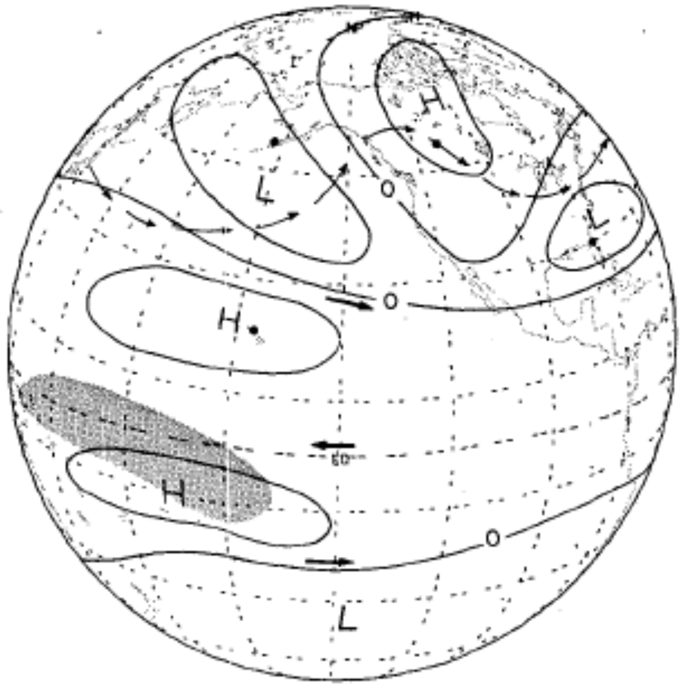

Understanding teleconnections: Gill 1980

Atmospheric response to near-equatorial heating

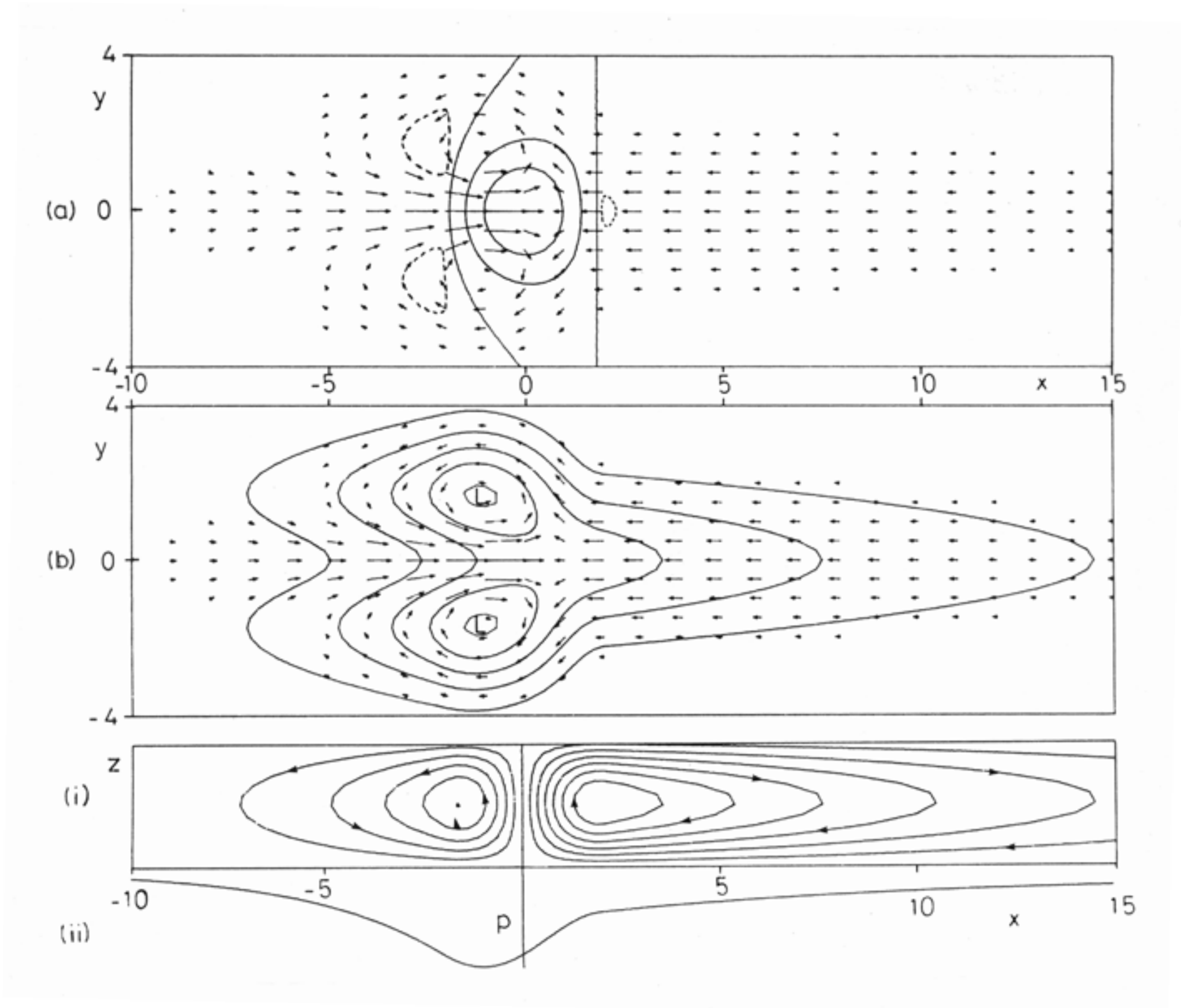

a) Near-surface wind and vertical motion

b) Near-surface wind and sea-level pressure

c) Motion in x-z plane along the Equator

Understanding teleconnections: Hoskins and Karoly 1981

Response to a tropical heat source (15N):

a) height (lon, z) at 18N
b) 300hPa vorticity
c) 300hPa height

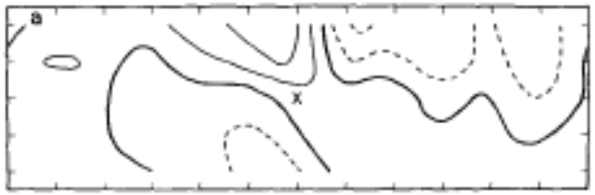

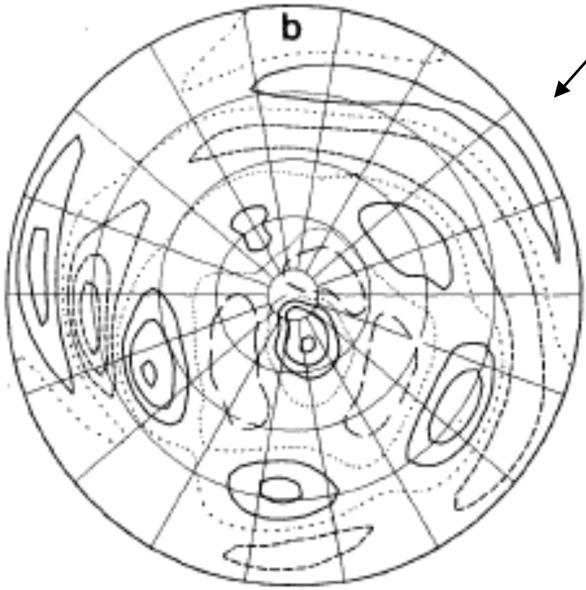

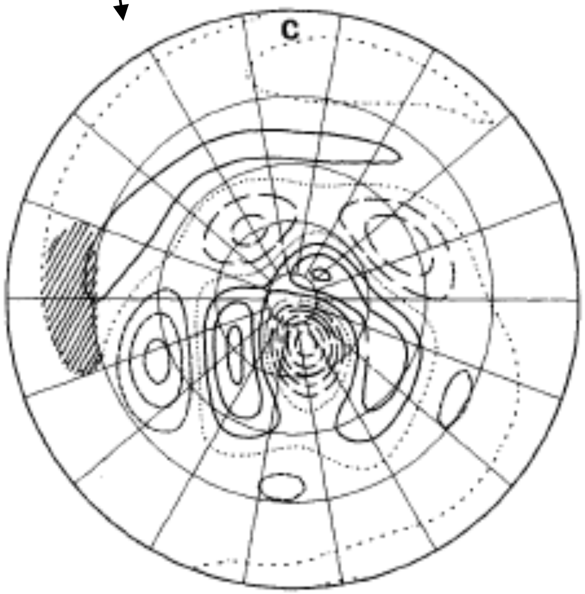

Understanding telecon.: Sardeshmukh and Hoskins 1988

Definition of Rossby wave source generated by near-equatorial heating

specification of the Rossby wave source S. If we are interested in the generation of Rossby waves, we are interested in the equation

$$\left(\frac{\partial}{\partial t} + \mathbf{v}_\psi \cdot \nabla\right)\zeta = S + F. \qquad (2)$$

Here $\mathbf{v}_\psi$ is the rotational wind associated with ζ. Comparing with (1) we see that we should write the total wind $\mathbf{v}$ in terms of its rotational and divergent components

$$\mathbf{v} = \mathbf{v}_\psi + \mathbf{v}_\chi$$

where $\nabla \cdot \mathbf{v}_\chi = D$. Then (1) may be written in the form of (2) but with

$$S = -\mathbf{v}_\chi \cdot \nabla\zeta - \zeta D. \qquad (3)$$

Understanding telecon: Simmons Wallace Branstator 1983

First barotropic normal mode at four times during a half-cycle:

East. Atlantic phase

PNA phase

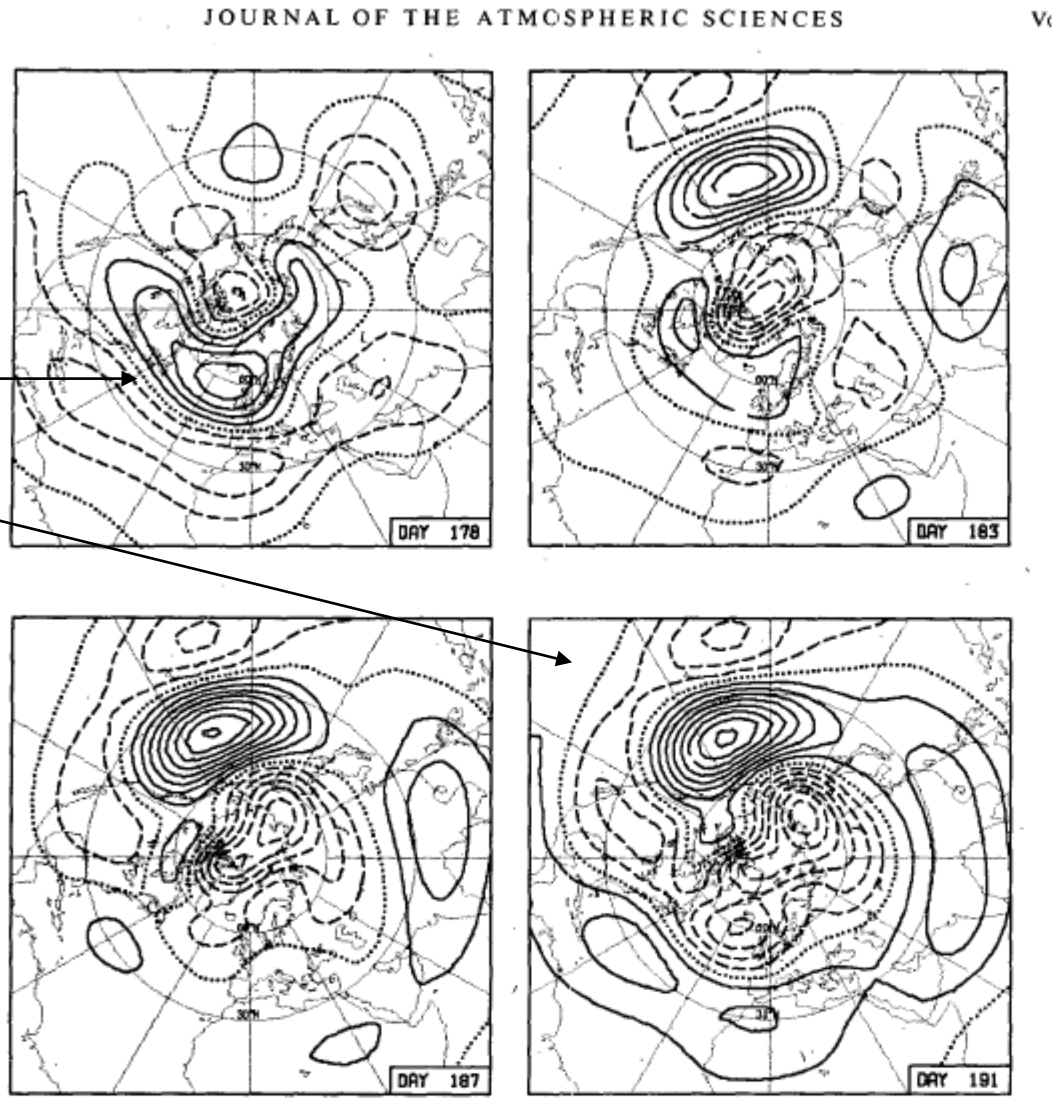

Recurrent flow patterns: examples

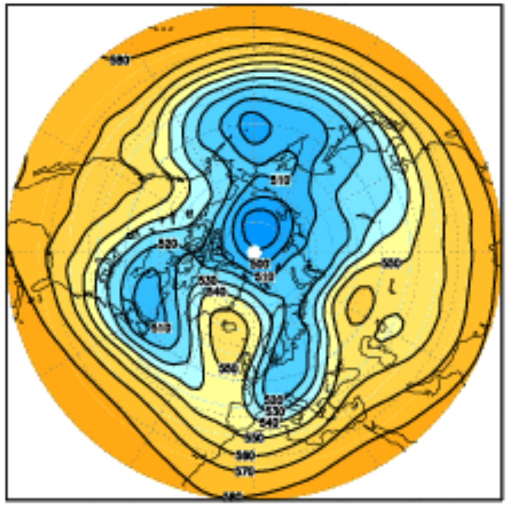

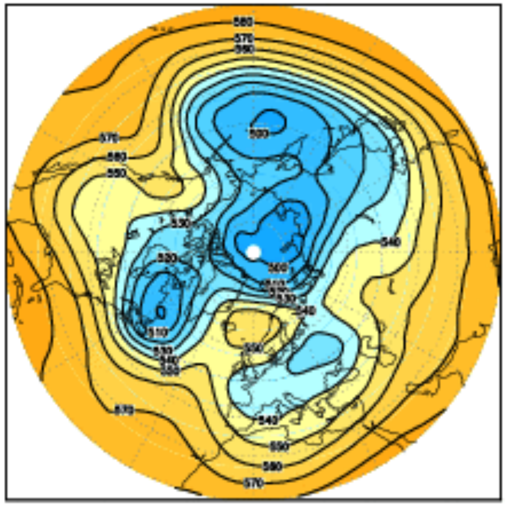

A sequence of 5-day mean fields of 500 hPa geopotential height during boreal winter …

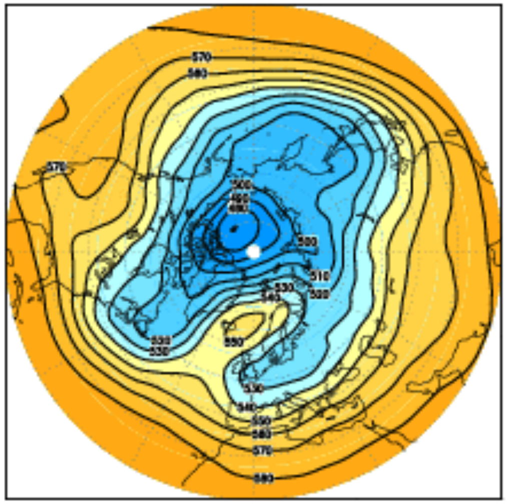

Recurrent flow patterns: examples

5-9 Jan
1985

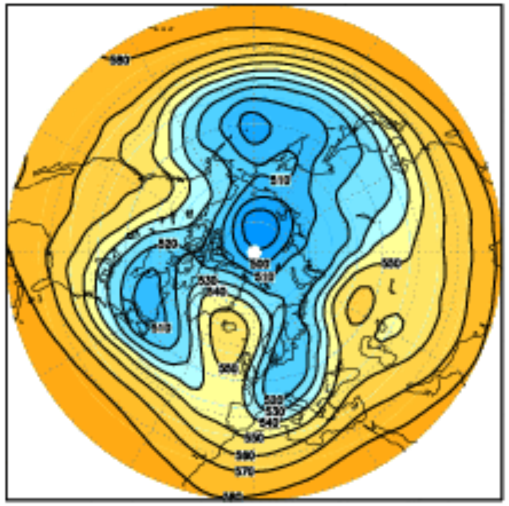

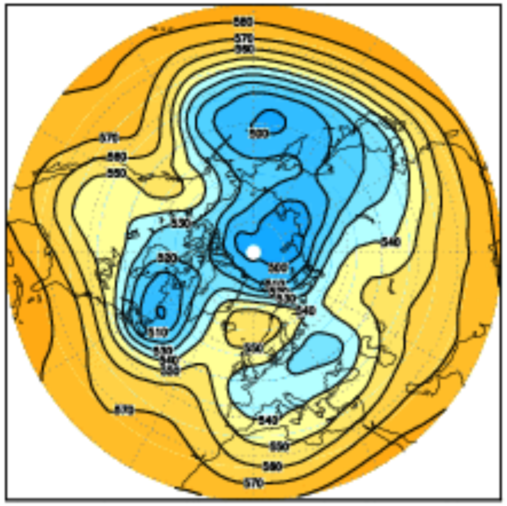

4-8 Feb
1986

... but each one occurred in a different winter !

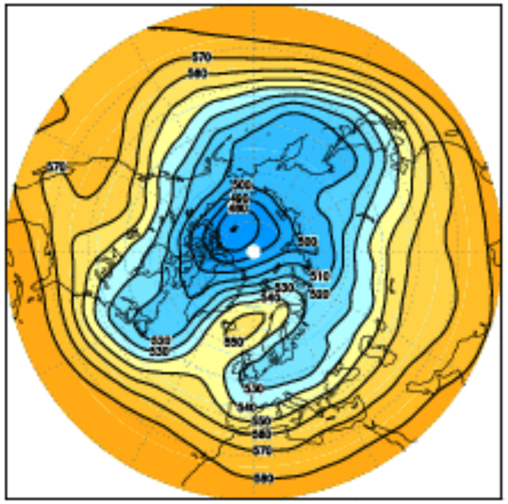

10-14 Jan
1987

Flow regimes in non-linear systems

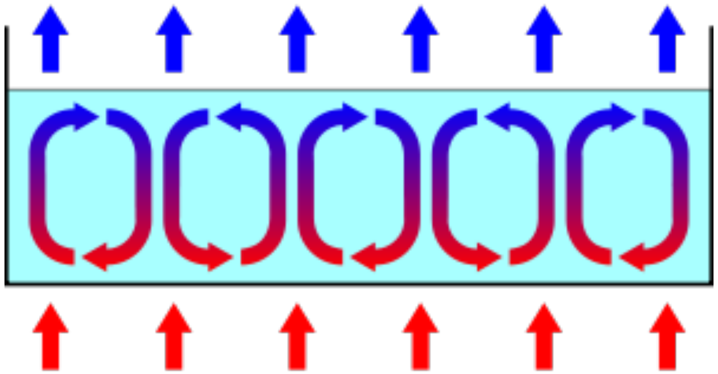

Lorenz (1963) *model of R-B convection*

- $dX/dt = \sigma\,(Y - X)$
- $dY/dt = -\,X\,Z + r\,X - Y$
- $dZ/dt = X\,Y - b\,Z$

Unstable stationary states

- $X = Y = Z = 0$
- $X = Y = \pm\,[\,b\,(r-1)]^{1/2}\ ,\ Z = r - 1$

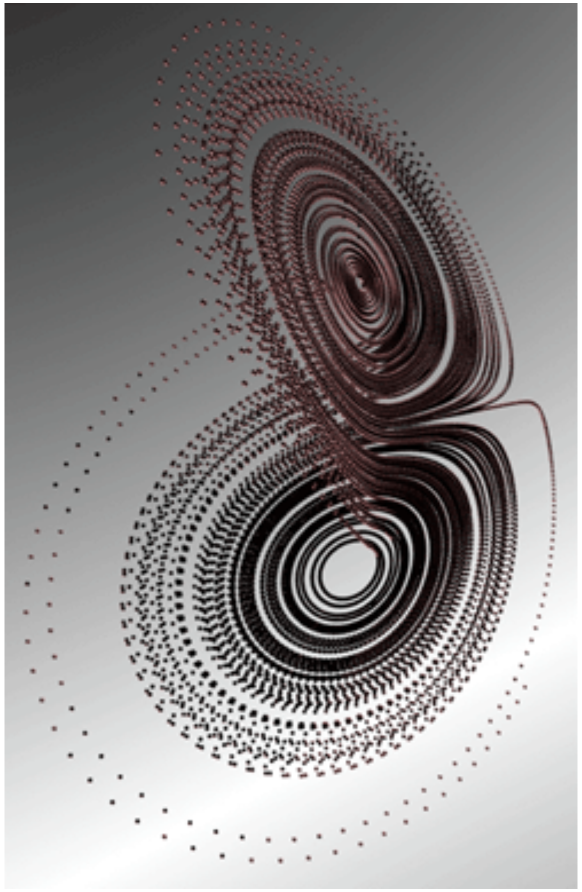

Regimes as quasi-stationary states

q : barotropic or quasi-geostrophic potential vorticity

$$\partial_t q = - V_\psi \cdot \mathit{grad}\, q - D\,(q - q^*)$$

steady state for instantaneous flow (multiple equilibria):

$$0 = - V_\psi \cdot \mathit{grad}\, q - D\,(q - q^*)$$

steady state for time-averaged flow (regimes):

$$0 = - \langle V_\psi \rangle \cdot \mathit{grad}\, \langle q \rangle - D\,(\langle q \rangle - q^*)$$
$$- \langle V'_\psi \cdot \mathit{grad}\, q' \rangle$$

Multiple equilibria: Charney and DeVore 1979

Multiple steady states of low-order barotropic model with wave-shaped bottom topography

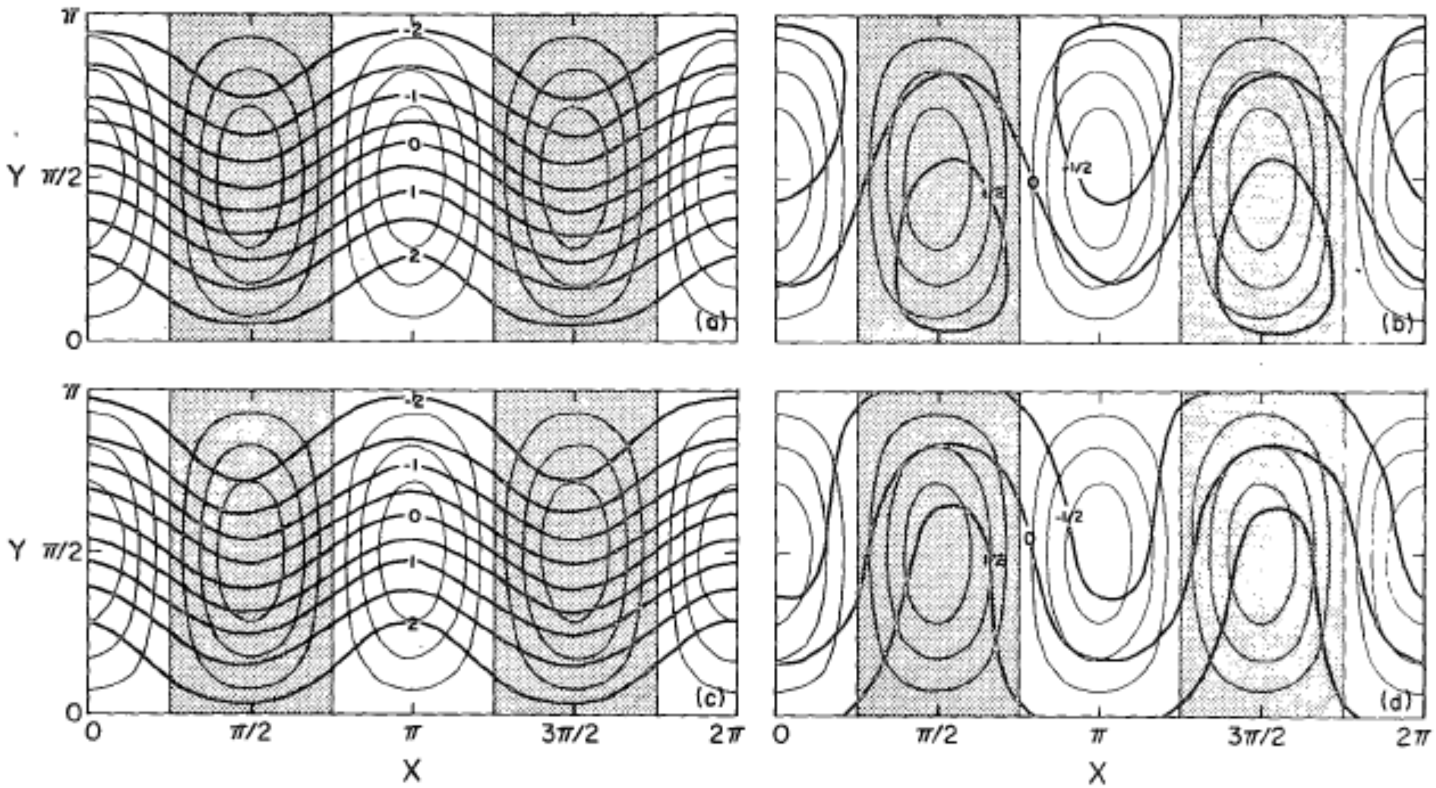

FIG. 4. Streamfunction fields of the stable first mode equilibria of a topographically forced flow for $k = 10^{-2}$, $L/a = 1/4$, $n = 2$, $h_0/H = 0.2$ and $\psi_A^* = 0.2$: for the spectral model above resonance (a) and slightly below resonance (b); and for the grid-point model above resonance (c) and slightly below resonance (d). The nondimensional topographic heights are shown with light lines; the contour spacing is 0.05 units, with negative regions shaded.

Papers on multiple equilibria and quasi-stationary states

Orographically forced models:

• **Charney and Straus 1980**: *Form-grad instability, multiple equilibria and propagating planetary waves in baroclinic, orographically forced, planetary wave systems*

• **Charney, Shukla and Mo 1981**: *Comparison of barotropic blocking theory with observation*

• **Legras and Ghil 1985**: *Persistent anomalies, blocking and variations in atmospheric predictability*

• **Benzi, Malguzzi, Speranza, Sutera 1986*****:*** *The statistical properties of the atmospheric general circulation: observational evidence and a minimal theory of bimodality*

Thermally forced models:

• **Mitchell and Derome 1983:** *Blocking-like solutions of the potential vorticity equation: their stability at equilibrium and growth at resonance*

Weather regimes: Reinhold and Pierrehumbert 1983

Hemispheric weather regimes arising from equilibration of large-scale dynamical tendencies and “forcing” from transient baroclinic eddies

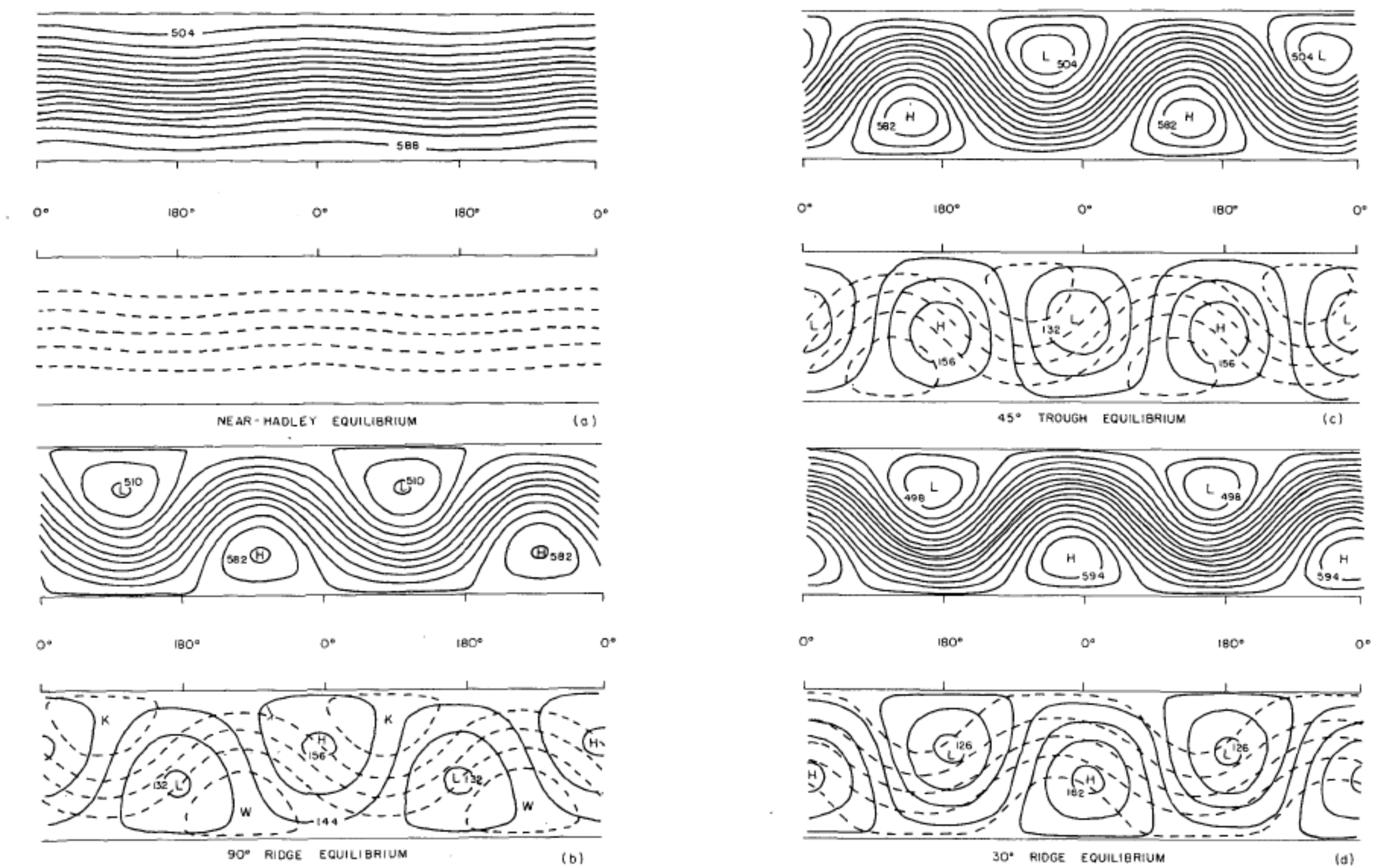

Regional regime behaviour: Atlantic/Pacific blocking

500 hPa geop. height

4−8 Feb. 1986

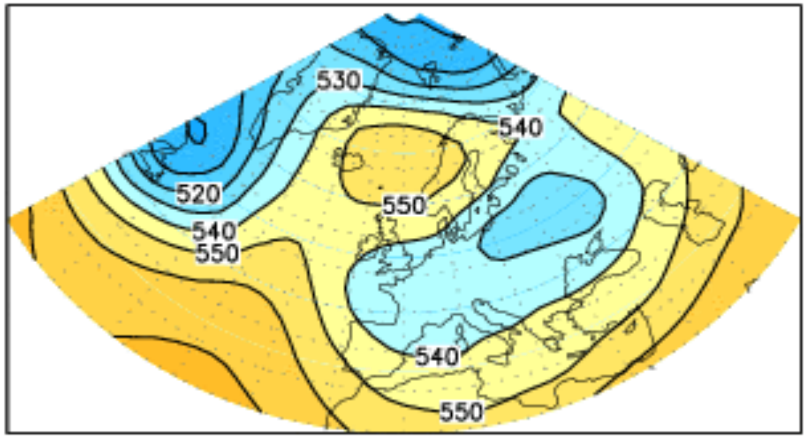

4−8 Feb. 1989

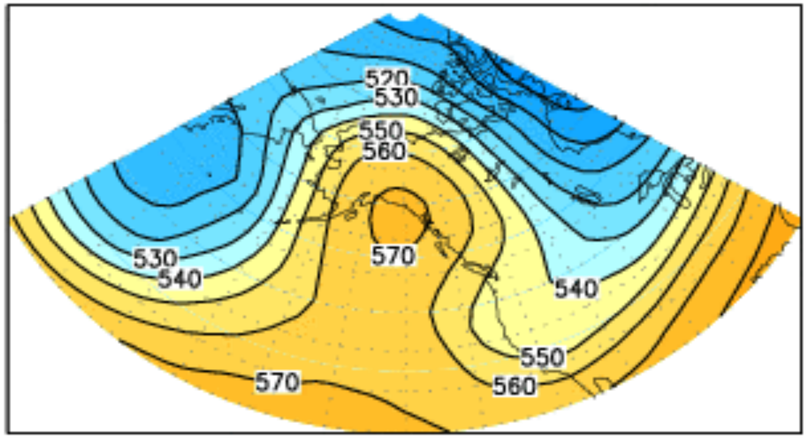

Eddy "forcing" of blocking: the Imperial College school

• **Green 1977**: *The weather during July 1976: some dynamical consideration of the drought*

• **Illari and Marshall 1983**: *On the interpretation of eddy fluxes during a blocking episode*

• **Shutts 1986**: *A case study of eddy forcing during an Atlantic blocking episode*

• **Haines and Marshall 1987:** *Eddy-forced coherent structures as a propotype of atmospheric blocking*

Regional regimes: Vautard and Legras 1988

Regional weather regimes arising from equilibration of large-scale dynamical tendencies and PV fluxes from transient baroclinic eddies

PSI LEVEL 1 ZONAL1

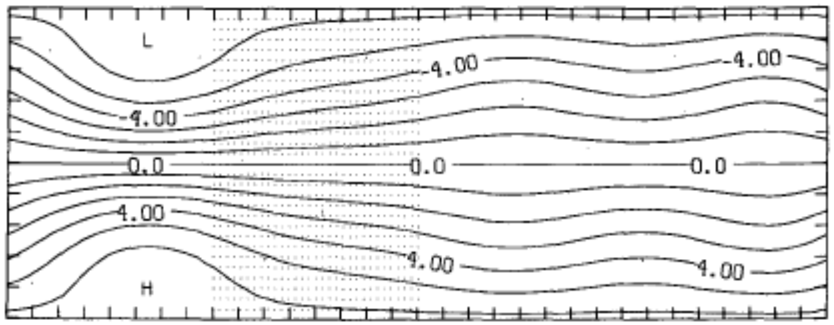

a

PSI LEVEL 1 ZONAL2

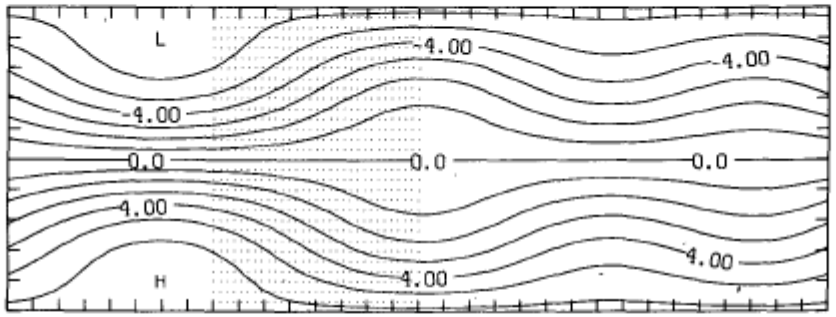

c

PSI LEVEL 1 BLOCK

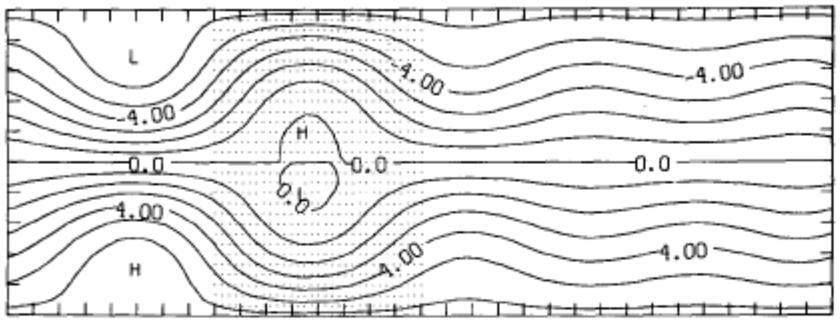

e

Low-frequency variability

of atmospheric planetary waves

Part II: impact on heat fluxes and transport

Franco Molteni

European Centre for Medium-Range Weather Forecasts

Net heat flux at ocean surface from ERA-interim

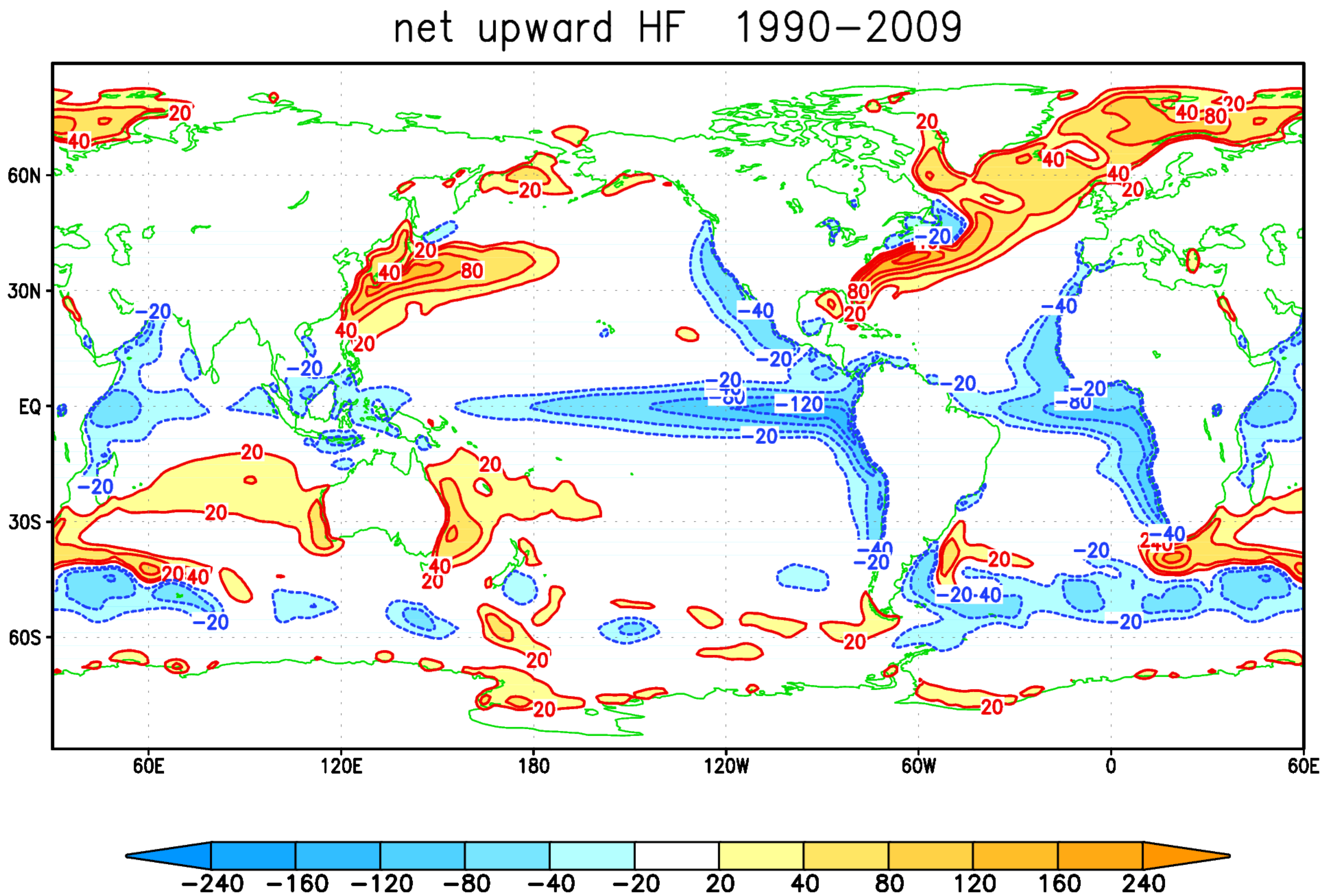

ENSO affects the heat fluxes in the Eq. Pacific

The El Niño - Southern Oscillation

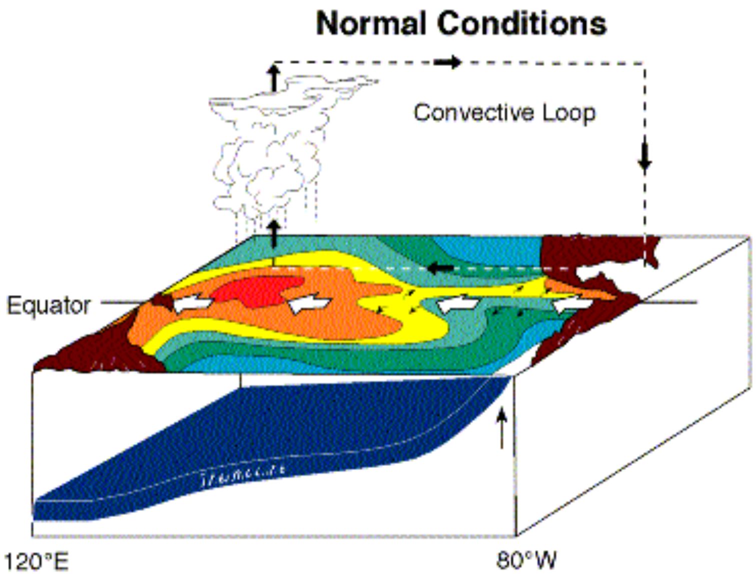

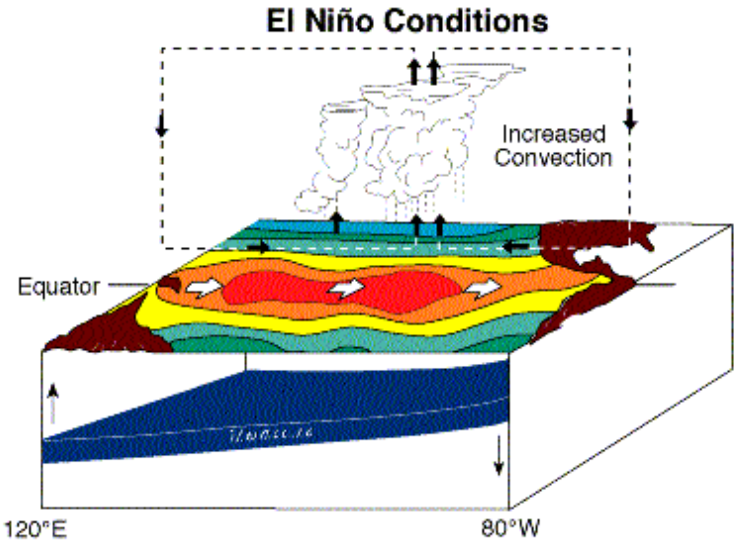

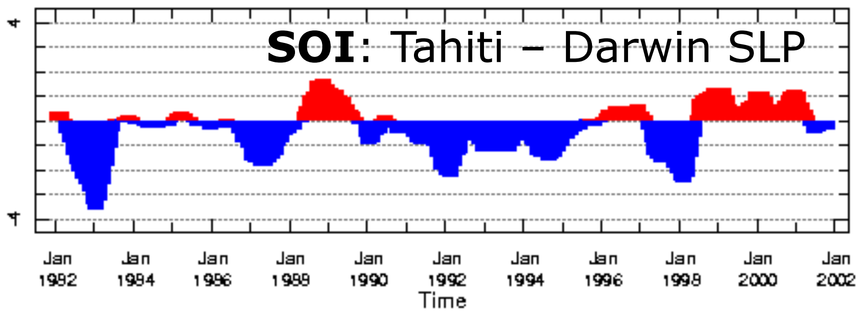

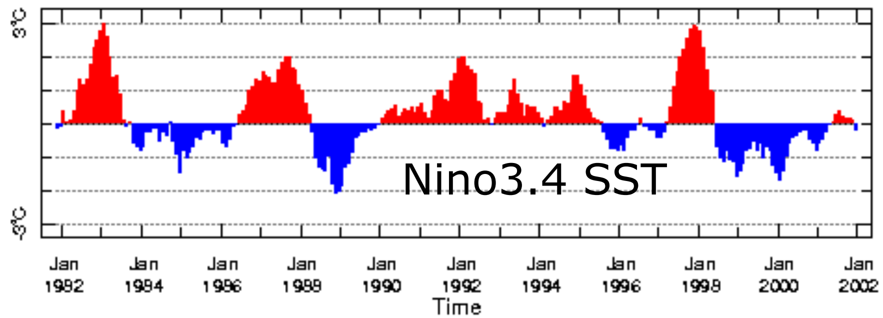

Thermal equilibration of planetary waves

Variability in the phase of planetary waves with respect to the surface temperature distribution in winter

- Mitchell and Derome (1983)
- Shutts (1987)
- Marshall and So (1990)

- *Equilibrated phase*: planetary waves ridges with higher temperature in the lower-troposphere are located over the warm oceans; surface heat fluxes and friction are reduced
- *Thermally forced phase*: planetary wave throughs (cold air) located on the western side of the oceans, strong temperature advection compensated by increased surface fluxes

Empirical variability patterns: EOFs and COWL

COWL (cold ocean – warm land) index after Wallace et al. (1995)

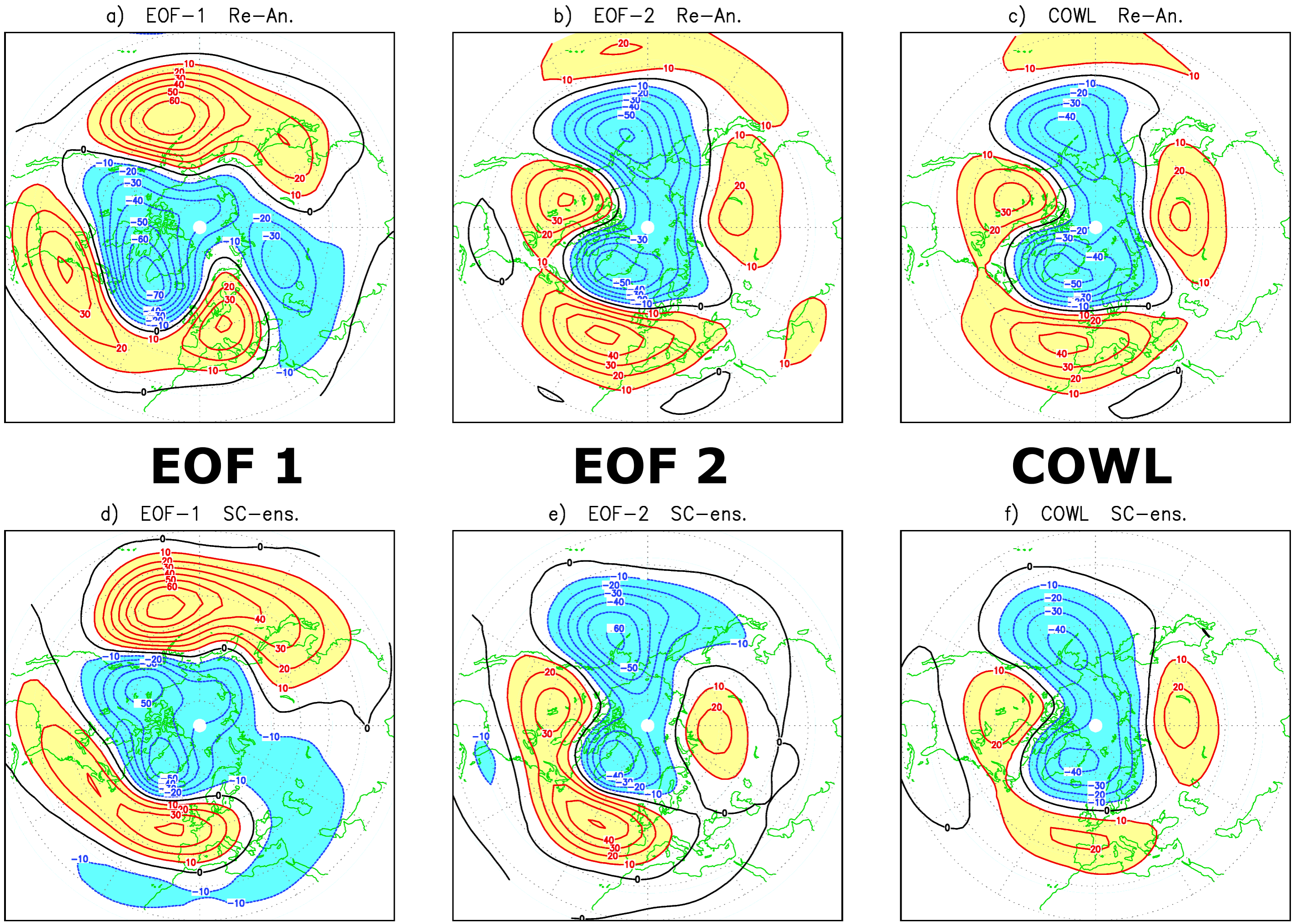

Z 500 hPa
JF 1950-2002

NCEP/NCAR
Re-Analysis

ICTP AGCM
simulations
forced by
HadISST

Definition of COWL-like variability from surface fluxes

- **Thermal-balance Wave index (positive in COWL phase)**:

  Zonal wanenumber-2 component of net surface heat flux (NSHF, positive upward) in the [45-70 N] latitudinal band:

  TW = NSHF [60W-30E] - NSHF [30E-120E] + NSHF [120E-150W] - NSHF [150W-60W] -

  Molteni, King, Kucharski and Straus, *Climate Dynamics 2010*

Regression of Z500/NSHF onto TW index

b) reg(gh_500, TW)

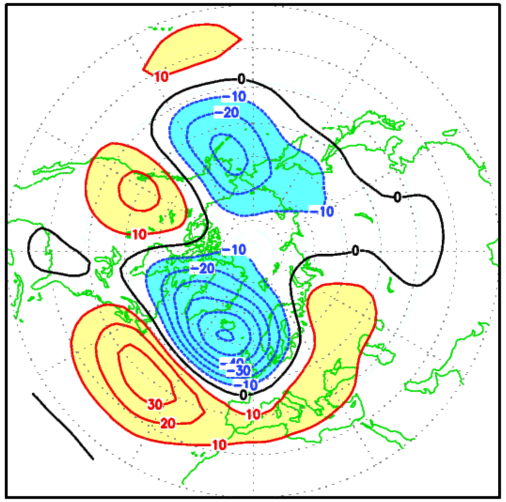

Z 500 hPa
JF 1950-2002

NCEP/NCAR
Re-Analysis

c) NSHF, negative TW　　　d) NSHF, positive TW

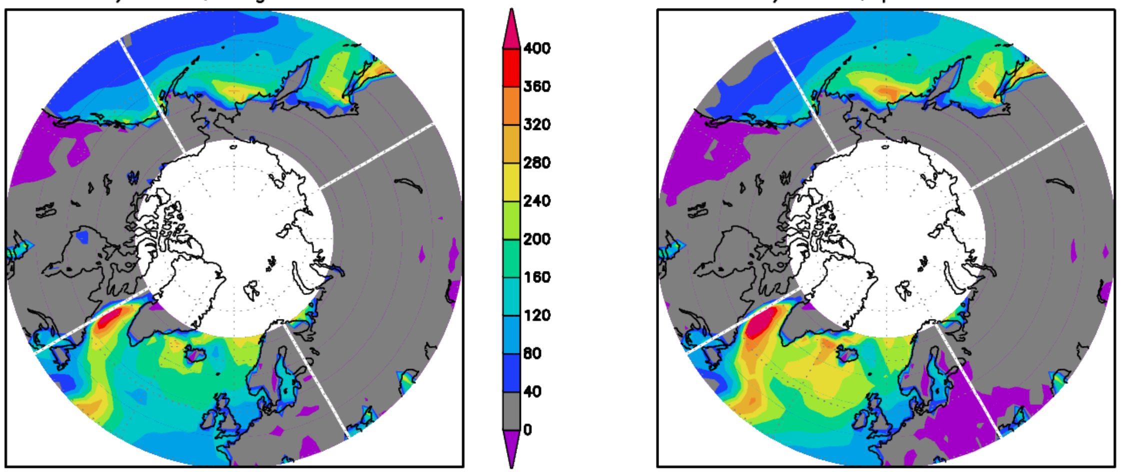

Net surface
heat flux
(+ upwards)

Is the TW mode relevant to decadal variability ?

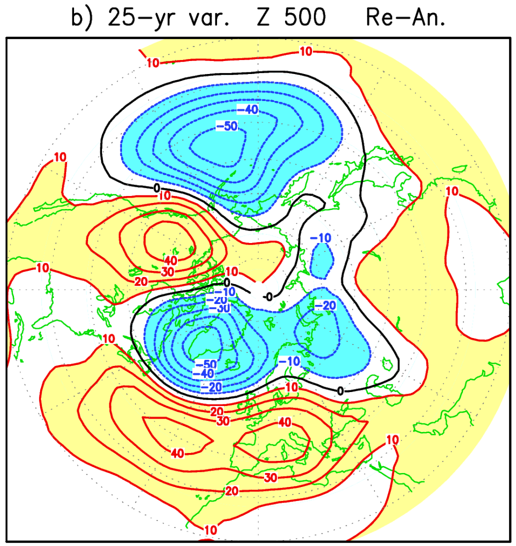

Z 500
(1976/2000)-
(1951/1975)

Z 500
TW composite
In NCEP
re-analysis

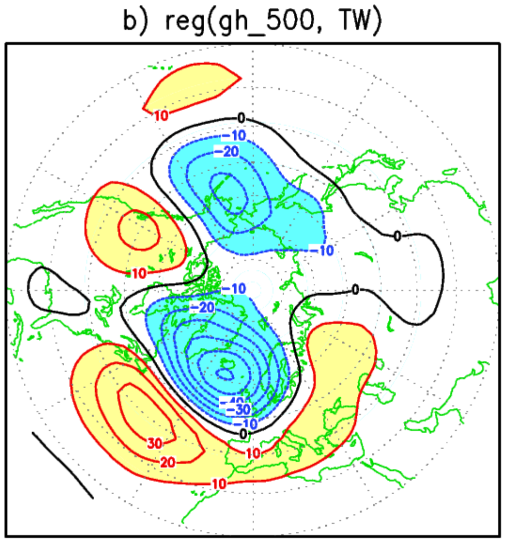

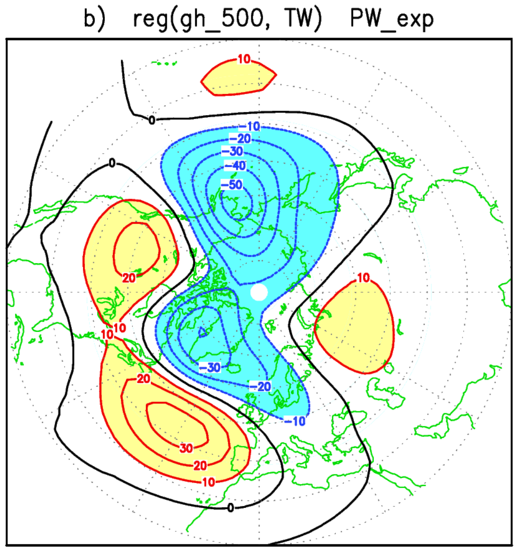

Z 500
TW composite
in ICTP model
simulation

Is it relevant to changes in ocean circulation?

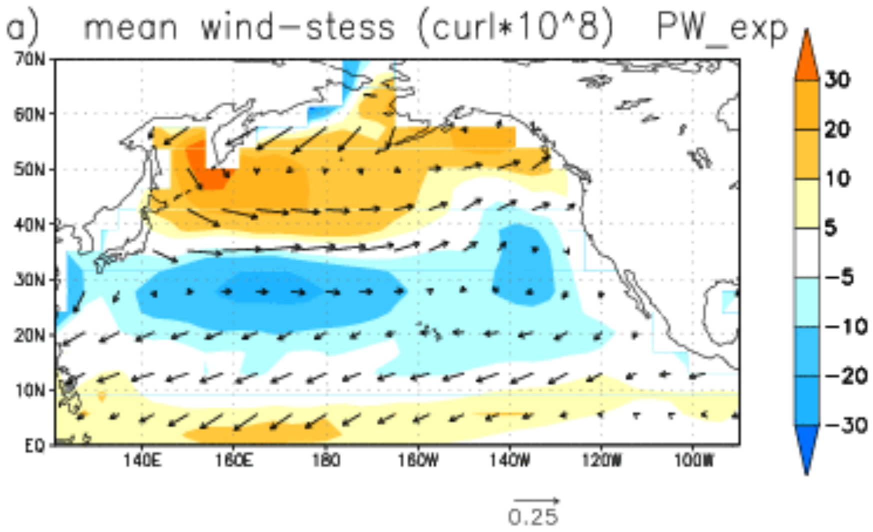

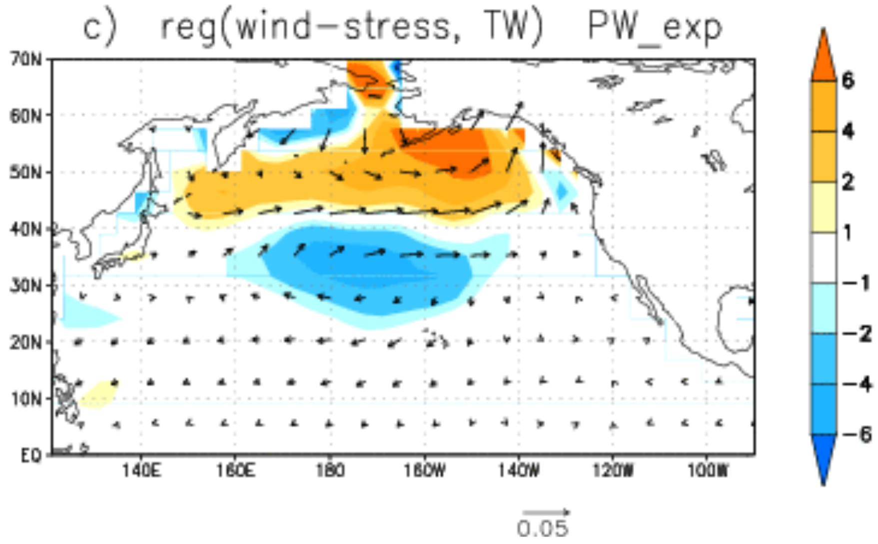

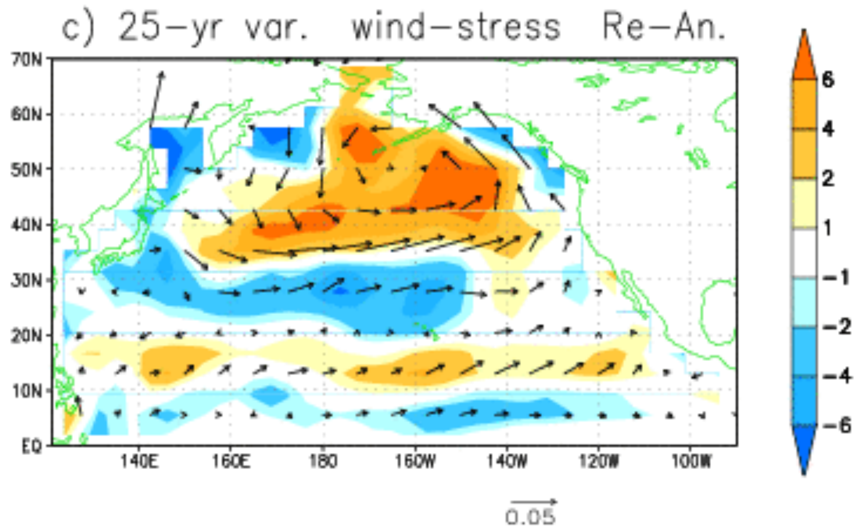

Decadal variability and climate change

NASA GISS surface air/sea temperature

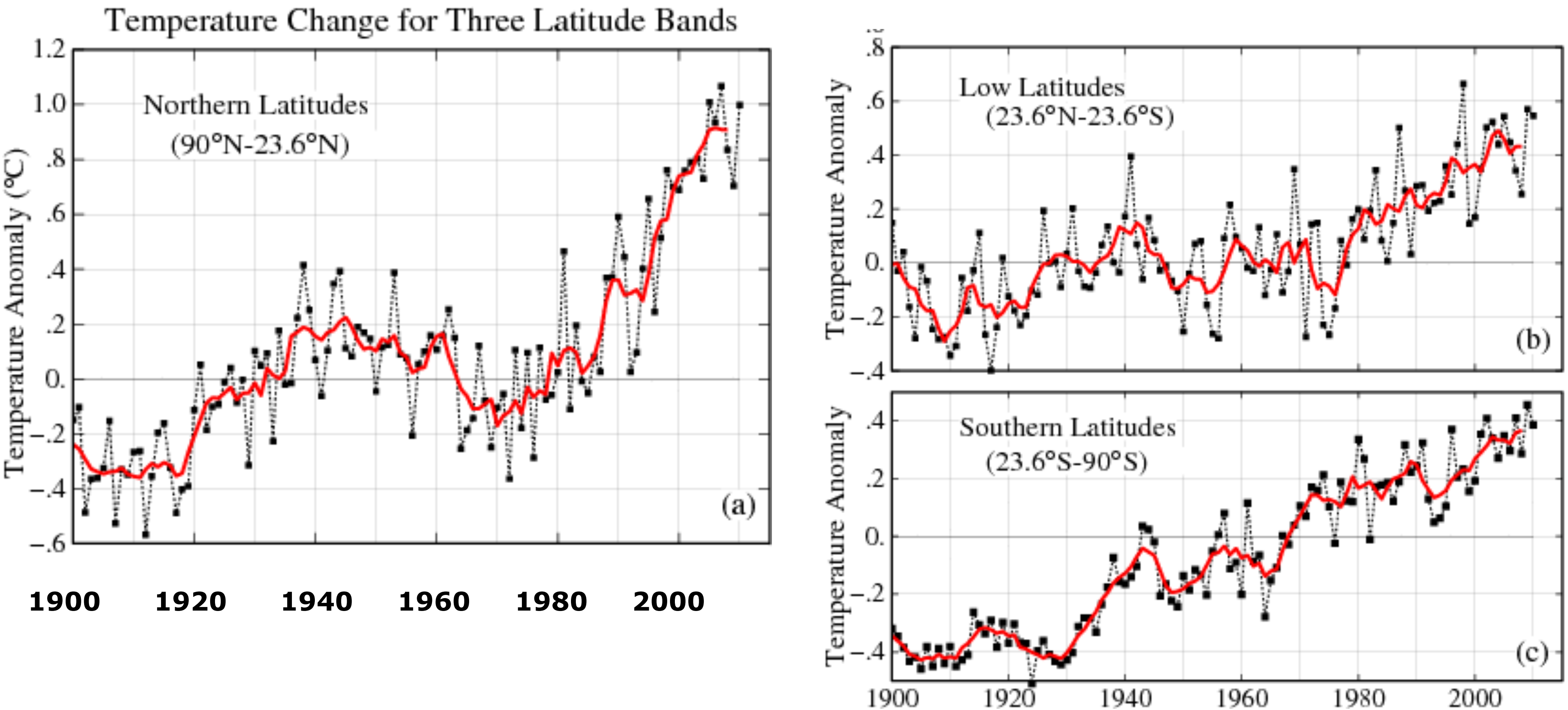

Atmospheric variability in the last two decades

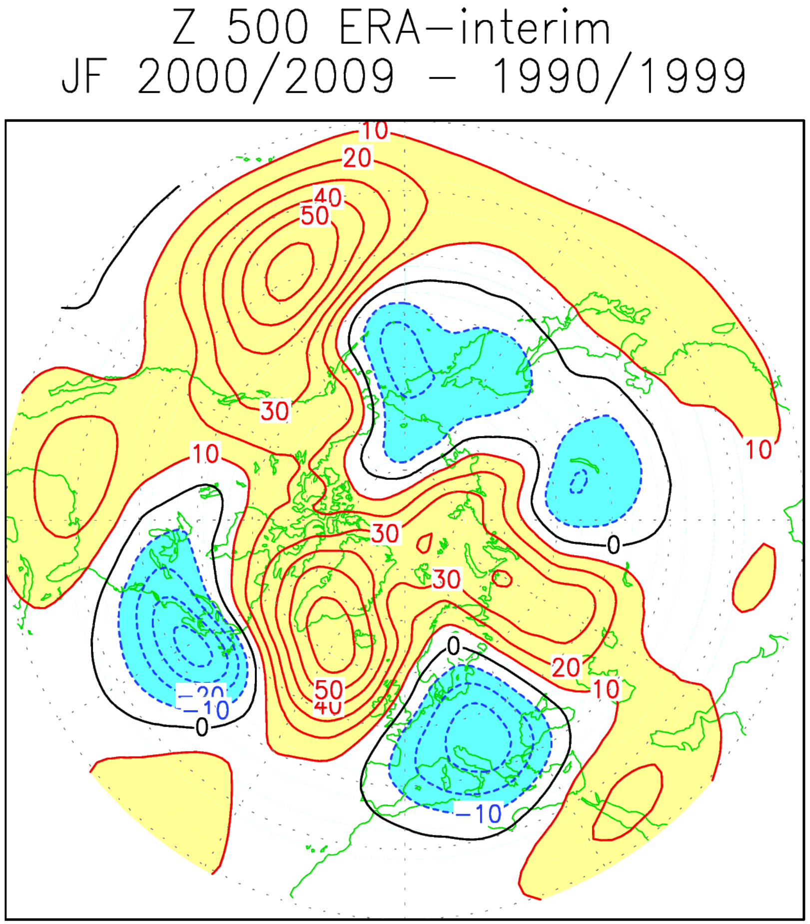

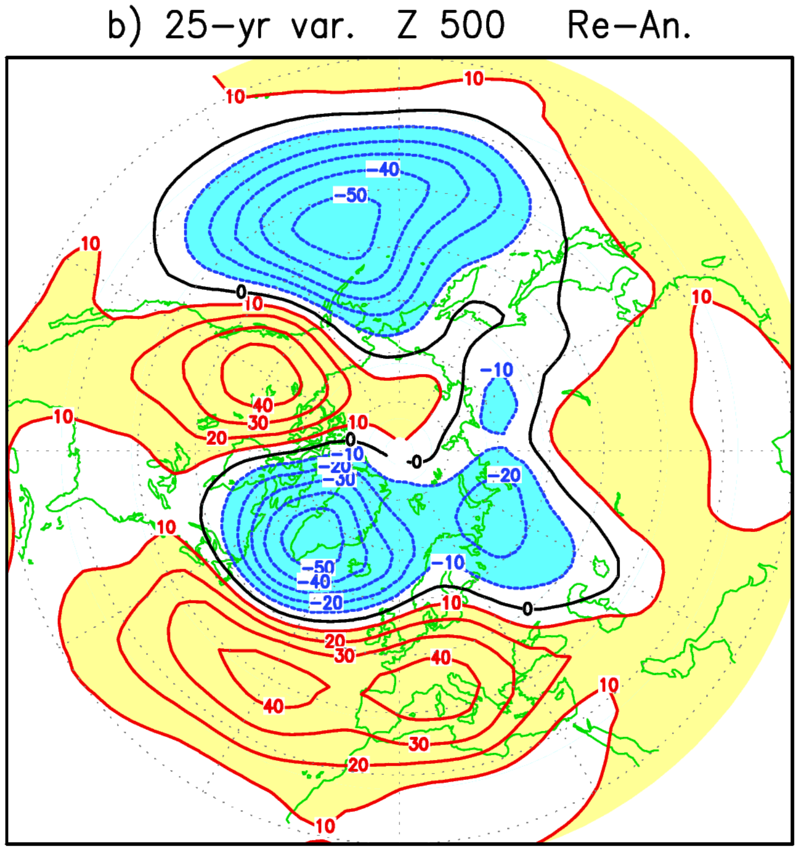

Inter-decadal SST variability in DJF

1976/00 - 1951/75

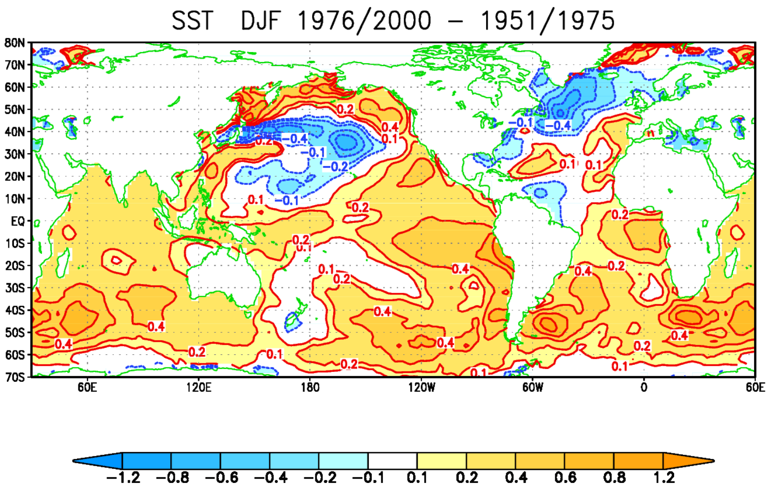

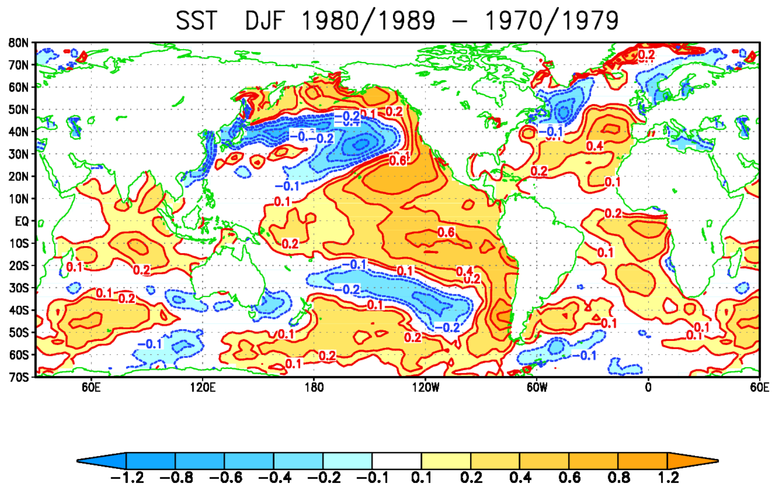

1980/89 - 1970/79

1990/99 - 1980/89

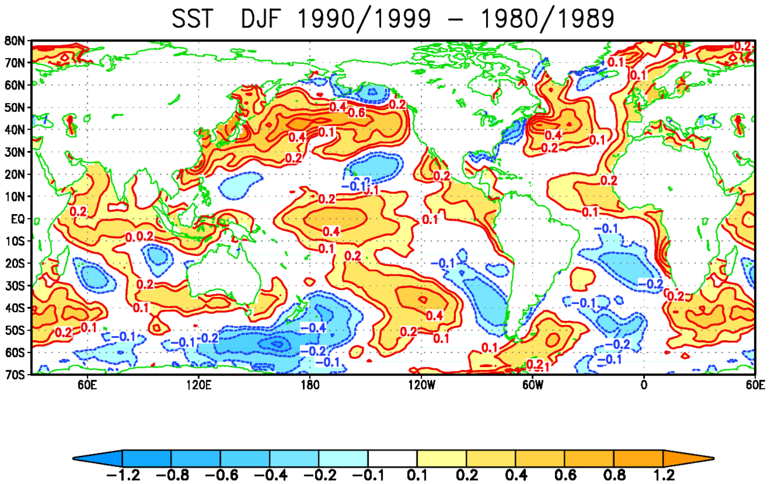

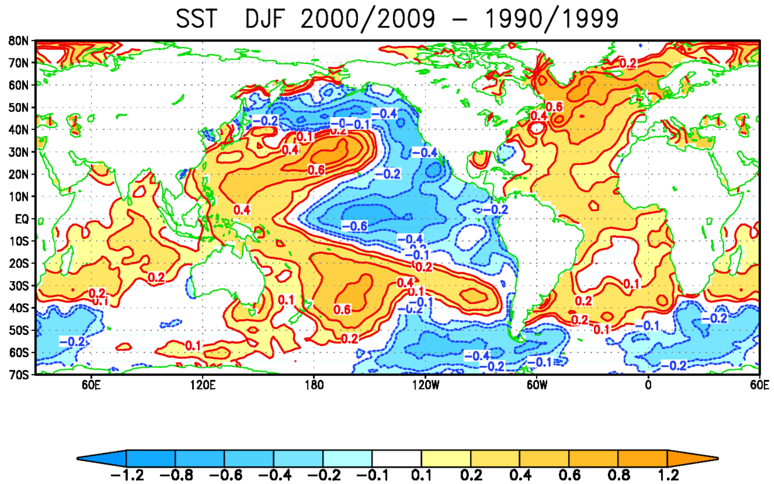

2000/09 - 1990/99

Decadal variability in surface fluxes and heat content

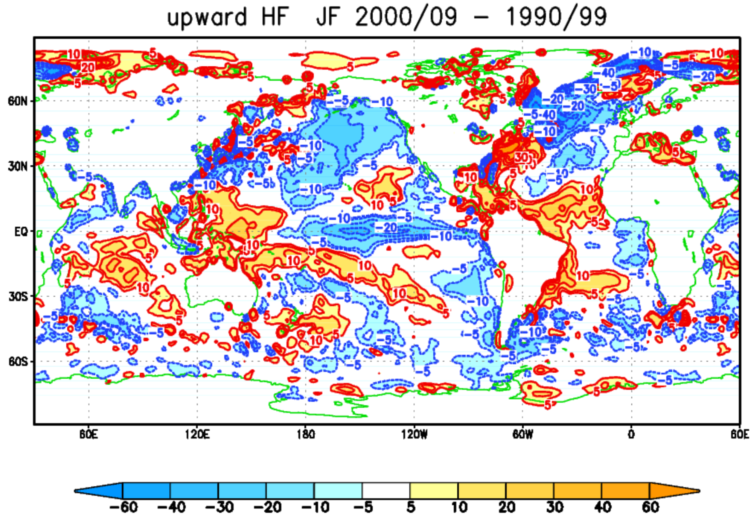

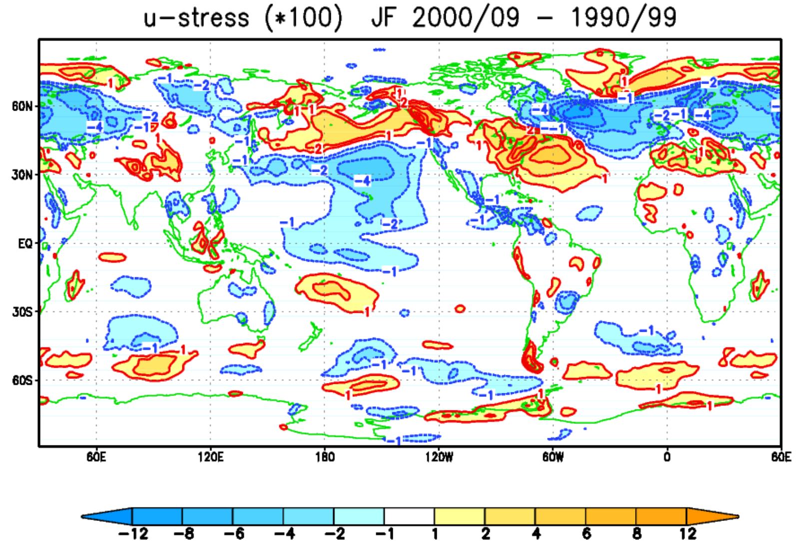

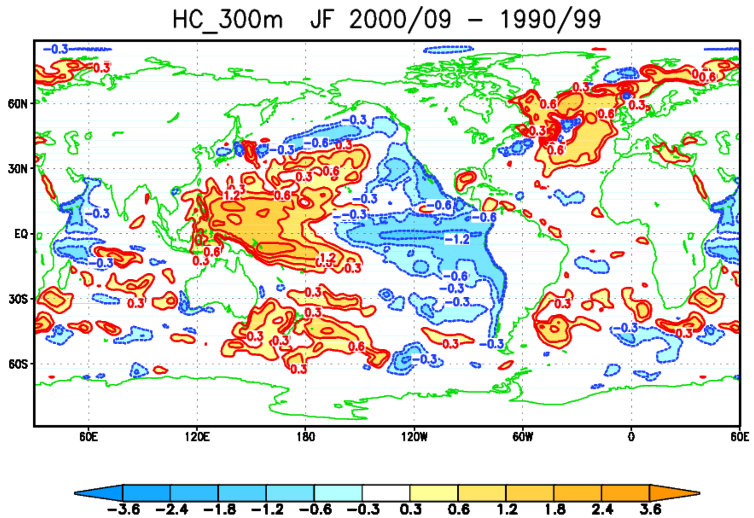

Surface fluxes from ERA-Interim

Ocean heat content in the top 300m from NEMOVAR-S4

Heat flux and heat content: winter and yearly means

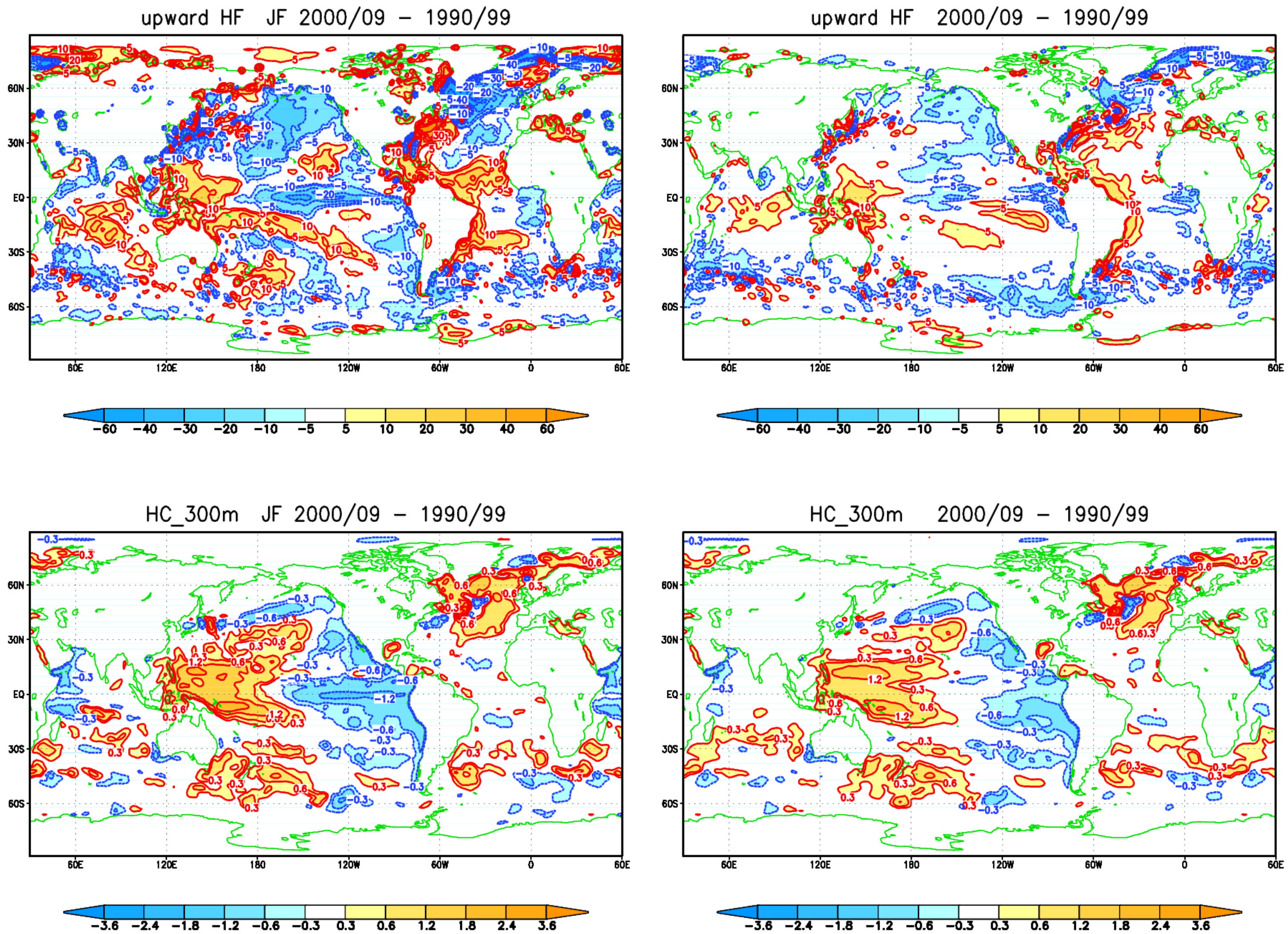

Summary

- Variability in planetary waves may be induced either by internal atmospheric dynamics (quasi-stationary responses to orographic and thermal forcing) or by teleconnections with coupled modes of tropical variability.
- Poleward heat transport by atmospheric planetary waves is not strongly dependent on the specific phase of waves.
- On the other hand, the amount of heat transferred from the ocean to the atmosphere in northern mid-latitudes is dependent on the phase of the planetary waves with respect to the land-sea distribution.
- The reversal of the phase of the COWL-like (TW) pattern in the last decade is consistent with reduced heat transfer in the northern oceans and increased ocean heat content in these regions.